Article

Not peer-reviewed version

The Metallogenic Chronology and Prospecting Indication of Tiechanghe Granite and Molybdenum Polymetal in Jiulong Area, West Sichuan, China

Shuang Yang , Hongqi Tan * , Zhongquan Li , Junliang Hu , Xinyan Wang , Daming Liu

Posted Date: 7 August 2024

doi: 10.20944/preprints202408.0432.v1

Keywords: Songpan-Ganzi; western Sichuan; molybdenite Re-Os; U-Pb Zircon; granite

 doi:10.20944/preprints202408.0432.v1

Article

The Metallogenic Chronology and Prospecting Indication of Tiechanghe Granite and Molybdenum Polymetal in Jiulong Area, West Sichuan, China

Shuang Yang [1,2], Hongqi Tan [1,3,*], Zhongquan Li [1], Junliang Hu [1], Xinyan Wang [4] and Daming Liu [1]

[1] College of Earth and Planetary Sciences, Chengdu university of technology, Chengdu 610059, China
[2] School of history, Geography and Tourism, Chengdu Normal university，Chengdu 611130, China
[3] Sichuan Geological and Mineral Resources Group Co., Ltd., Chengdu 610016, China;
[4] Sichuan Xinjinlu Group Co., Ltd., Deyang 610507, China
* Correspondence: Correspondence: hongqitan@163.com

Abstract: The Songpan-Ganze Orogenic Belt (SGOB) is bounded by the South China, North China, and Qiangtang blocks and forms the eastern margin of the Tibetan Plateau. The Tiechanghe granite is located at the junction of the southeast margin of the SGOB and the western margin of the Yangtze Block. To elucidate the genetic relationship between the Tiechanghe granite and the surrounding molybdenum deposits in Western Sichuan, in this study, we conducted U-Pb zircon and molybdenite Re-Os isotopic dating. The results indicate that the Tiechanghe granite predominantly consists of monzogranite, with minor occurrences of syenogranite, while the molybdenum deposits are mainly found in skarn and quartz veins. The laser ablation inductively coupled plasma mass spectrometry (LA-ICP-MS) U-Pb zircon ages of the Tiechanghe granite range from 162.9 ± 0.7 Ma to 163.4 ± 0.6 Ma, and the zircon LA-ICP-MS U-Pb age of the pegmatite veins is 164.1 ± 0.9 Ma. These ages are consistent with the weighted average Re-Os age of the Ziershi molybdenite (160.3 ± 1.6 Ma) within the error margins. These findings and previously obtained magmatic and metallogenic ages for the region suggest that a magmatic and mineralization event involving granite, molybdenum, tungsten, and copper occurred at around 162–164 Ma in the study area. This discovery broadens the exploration perspective for mineral resources in the Jiulong area of Western Sichuan and the entirety of Western Sichuan.

Keywords: Songpan-Ganzi; western Sichuan; molybdenite Re-Os; U-Pb Zircon; granite

1. Introduction

Granite, broadly referred to as granitic rocks, is a crucial component of continental crustal rocks. It plays a significant role in studying the formation and evolution of the continental crust and holds substantial scientific significance in research on the genesis of endogenous metal deposits. Additionally, granite possesses strategic value for national economic development [1–5]. In the western Sichuan region, Indosinian to Yanshanian granites are distributed in areas such as Eastern Tibet Jiangda, Yidun Island Arc Belt, Kangding Songlinkou-Tagong, Maerkang, and Jiulong Fangmaping-Sanyanlong, and they have U-Pb zircon ages ranging from 225 to 205 Ma. These granites are primarily S-type, with minor occurrences of I-type granites [6–27]. The Early Yanshanian (166–150 Ma) granites are only exposed in the Jiulong area in regions such as Tiechanghe, Xinhuoshan, Qiaopengzi-Landiao, and Huajiaoping granite [28–39]. Recent studies in the Danba area have reported magmatic and metallogenic ages of 153–177 Ma, which are considered to be metamorphic ages [40,41]. It is speculated that magmatic activity during the Yanshanian period may have occurred at the junction of the eastern margin of the Songpan-Ganzi Block and the western margin of the Yangtze Block, and such rocks are currently exposed only in the Jiulong area. These findings provide an opportunity to study the tectonic evolution of the Songpan-Ganzi Block during the Yanshanian.

 doi:10.20944/preprints202408.0432.v1

The Jiulong area in western Sichuan is rich in mineral resources related to Yanshanian granites, including rare metals (Li and Be), tungsten, and molybdenum. Representative deposits include the Daqiangou Li-Be deposit, the Daniuchang tungsten-molybdenum deposit, and the Ziershi copper-molybdenum deposit. Through laser ablation inductively coupled plasma mass spectrometry (LA-ICP-MS) U-Pb zircon dating of the Tiechanghe granite and Re-Os dating of molybdenite, in this study, we precisely determined the magmatic and metallogenic ages of the Ziershi Cu-Mo deposit. We explored the genesis of the deposit and summarized the metallogenic patterns, providing significant insights for guiding mineral exploration in the Jiulong area in western Sichuan.

2. Regional Geological Background

The Jiulong area in western Sichuan is located in the southern part of the Songpan-Ganzi orogenic belt and is bordered by the Ganzi-Litang fault zone to the west and the Longmenshan-Jinpingshan orogenic belt to the east (Figure 1a,b). The Xianshuihe fault is located to the north-northeast, and the Muli-Yanyuan arcuate structural belt is located to the south. The Triassic Xikang Group strata are extensively exposed in the study area [42,43], primarily including schist and slate. The Ordovician-Carboniferous strata are only exposed in the southern part of the study area, including schist, metagraywacke, and quartzite. The western part of the study area includes the Yulongxi fault zone, which is northeast-southwest trending and is connected to the Ganzi-Litang fault zone in the west and aligned with the long axis of the magmatic body. The central part is characterized by north-south trending faults, the eastern part by the Qingna fault zone, and the southern part by detachment faults within the dome structure (Figure 1b). Additionally, the area exhibits a complex fold structure with a continuous distribution of anticlines and synclines.

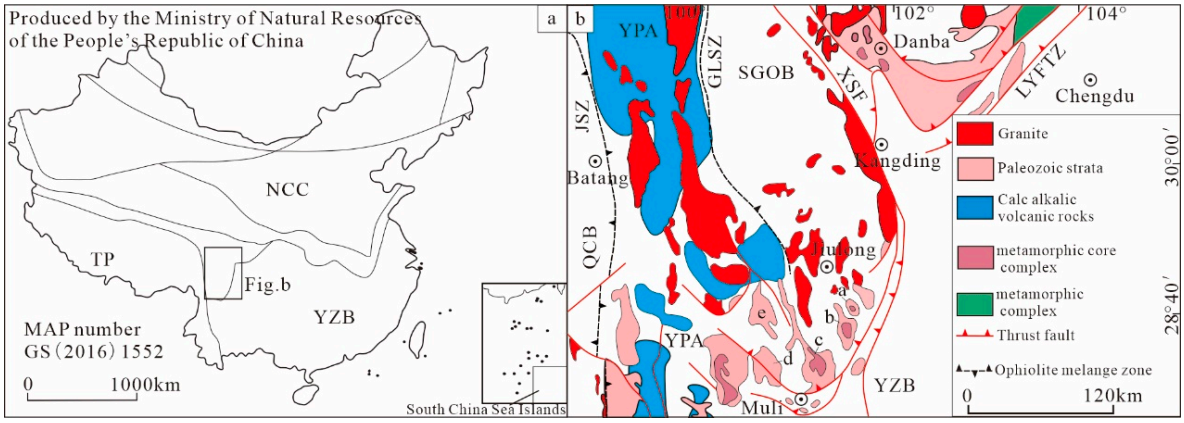

Figure 1. Geological map of the eastern margin of the Tibetan Plateau, showing the Longmenshan–Yanyuan Foreland Thrust Zone (LYFTZ) and the distribution of tectonic domes. Tectonic units: the Songpan–Garze Orogenic Belt (SGOB); the Yidun Paleozoic Arc (YPA); and the Qiangtang–Changdu Block (QCB). Major sutures and faults: the Jingshajiang Suture Zone (JSZ); the Garze–Litang Suture Zone (GLSZ); the Xianshuihe sinistral Strike-slip Fault (XSF). Major metamorphic dome: Taka dome(A), Jianglang dome (B), Changqiang dome (C), Qiasi dome (D), Tangyang dome (E).

Controlled by tectonics, the Jiulong area experienced two periods of granite intrusion: the Indosinian period (220–205 Ma) and the Yanshanian period (165–160 Ma) (Figure 2). The Indosinian granites (220–205 Ma) include the Lanniba, Yangfanggou, Sanyanlong-Fangmaping, Galazi, and Dichishan granites [17,25,38,39,44,45]. The Yanshanian granites (165–150 Ma) include the Xinhuaoshan (also known as Wenjiaping), Tiechanghe (also known as Wulaxi), and Qiaopengzi-Landiao granites [24,26,28–36]. The early metamorphism in this region was primarily regional metamorphism (low greenschist facies), which was followed by contact metasomatism around the granites. Only the Jianglang and Taka domes exhibit high greenschist to low amphibolite facies metamorphism [34].

 doi:10.20944/preprints202408.0432.v1

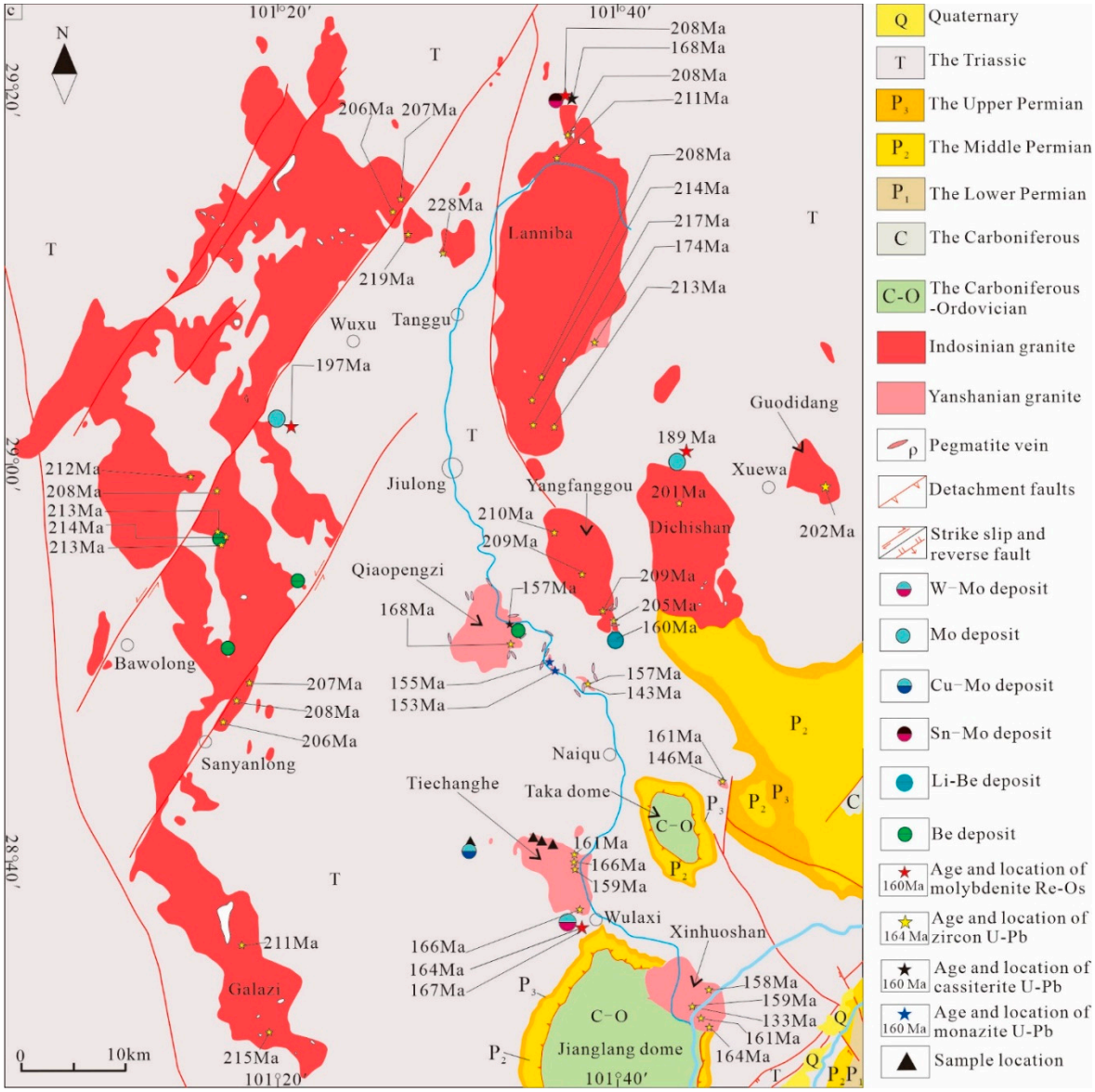

Figure 2. Geologic map of the Jiulong region and its adjacent areas in western Sichuan (after literature [10–15,17,22,24–39,44,45]).

Moreover, this region contains copper-zinc, lithium-beryllium, lead-zinc, and tungsten-molybdenum deposits [34,35,46–50]. Except for the Liwu copper-zinc deposit, which has two mineralization ages (343 Ma and 153–151 Ma) [48,49], the ages of the other deposit are constrained within 166–150 Ma and 180–200 Ma [24–26,34,35]. In summary, the Jiulong area in western Sichuan is rich in Cu-Pb-Zn-W-Mo and rare metal deposits, and the mineralization ages are concentrated in the Indosinian and Yanshanian periods [24].

The Tiechanghe pluton (also known as the Wulaxi pluton) is located at the confluence of the Tiechanghe and Jiulonghe rivers. This pluton exhibits intrusive contact with the surrounding rocks and steep outward dipping contact interfaces. The surrounding rocks are Middle Triassic Zagashan Formation metamorphosed sandstone, as well as slate interbedded with marble, and the periphery includes a thermal contact metamorphic zone that varies from 50 to 100 m in size. Altered rocks include actinolite-diopside-albite rock, biotite-quartz hornfels, hornfelsed sandstone, mica schist, and skarn. Two sets of joints are developed within the pluton: one set trends 310–330°∠50–60°, and the other set trends 55–70°∠65–75°, with straight joint surfaces and no mineral filling observed. Pegmatite veins of varying scales are distributed within the pluton. The Tiechanghe pluton is composed of syenogranite and monzogranite. The central part consists of medium-grained monzogranite, transitioning outward to medium-grained syenogranite and fine-grained syenogranite.

 doi:10.20944/preprints202408.0432.v1

3. Deposit Geology

Molybdenum occurrences have been discovered around the Tiechanghe pluton, including the Wulaxi Daniuchang Mo-W deposit and the Ziershi Cu-Mo deposit.

3.1. Daniuchang Mo-W Deposit

The stratigraphy of the deposit area belongs to the Zagashan Formation (Triassic Xikang Group), primarily composed of metamorphosed sandstone, slate, and interbedded marble. The structural setting of the deposit is simple, with only a few gentle small-scale folds observed. The area underwent regional metamorphism in its early stages, followed by thermal contact metamorphism due to the intrusion of the granite pluton, including hornfels, skarn, schist, and marble. These rocks are generally gray-green and exhibit granular metamorphic textures and massive or banded structures. The main minerals present are grossular, andradite, diopside, hedenbergite, and vesuvianite, minor minerals such as epidote, clinozoisite, tremolite, mica, calcite, tourmaline, fluorite, and metallic minerals, including hematite, sphalerite, and pyrrhotite.

Four ore bodies have been identified in this deposit, which are primarily hosted in skarn and quartz veins and exhibit stratiform, stratiform-like, and lenticular morphologies. Ore bodies I-III are located in the central part of the deposit and are the largest skarn belt in the area, with an exposed length of approximately 1000 m and a width of more than 10 m. The general orientation of the ore body is 120°∠8°, and it exhibits stratiform and lenticular occurrences within the layered skarn, which is consistent with the skarn's orientation. The mineralization features scheelite disseminated within the skarn. The lithology is mainly composed of diopside skarn and diopside-clinozoisite skarn, and the surrounding rocks are schist, phyllite, and marble. The grade of the scheelite ore bodies ranges from 0.07% to 0.52% (average of 0.22%), and it has a total thickness of 6.37 m. Ore body IV features an upper quartz vein-type molybdenite ore body and a lower skarn-type molybdenite ore body. The exposed surface has a width of 2–3 m, and it exhibits stratiform, stratiform-like, and lenticular morphologies. The ore body generally trends east-west with an orientation of 131°∠10°, its thickness ranges from 2.45 to 7.28 m, and the molybdenite ore grades range from 0.14% to 0.27% (average of 0.17%). The alteration of the wall rocks includes skarnification and silicification, and the main mineral assemblages include diopside + tremolite + hornblende, clinozoisite + tremolite + secondary amphibole + calcite, and biotite + chlorite + epidote + vesuvianite. The main ore minerals are scheelite and molybdenite, and the gangue minerals include calcite, biotite, chlorite, and epidote. Seven molybdenite samples from the deposit yielded an Re-Os weighted average age of 166.8 ± 1.7 Ma (mean squared weighted deviation (MSWD) = 0.90), which is consistent within error margins with the magmatic age of the Tiechanghe granite (166.0 ± 0.9 Ma). This indicates that the magmatism and mineralization occurred during the early Yanshanian [35].

3.2. Ziershi Molybdenum Deposit

The Ziershi molybdenum deposit is a newly discovered deposit located approximately 2 km north of the Tiechanghe pluton in Wulaxi Township in the Jiulong region. The southern part of the mining area is dominated by the exposure of the Tiechanghe monzogranite. The ore-hosting wall rock belongs to the Lower Triassic Bozigou Formation, primarily including gray to dark-gray biotite-hornblende schist. The mining area covers approximately 6 km², is distributed in patches, and exhibits sporadic iron staining and hydroxyl-type anomalies. These anomalies are mainly caused by ferruginous and carbonate alterations of the strata, suggesting the influence of granite veins or concealed plutons and indicating that they are mineralization-related anomalies. The Ziershi copper-molybdenum deposit is mainly quartz vein type. Only one ore body has been identified in the mining area, which exhibits stratiform, stratiform-like, and lenticular occurrences. The ore body has an exposed length of about 300 m, a width of 1–3 m, and a trend of 310°. The surface of the quartz vein contains abundant malachite, spotty chalcopyrite, and cluster-like or flaky molybdenite (Figure 3), with strong limonitization. The general orientation of the ore body is 24°∠65°, which is consistent with that of the surrounding rock. The surrounding rock is grayish-white with a slightly greenish tint

 doi:10.20944/preprints202408.0432.v1

and exhibits granular metamorphic textures and massive to banded structures. The main mineral is molybdenite, and minor metallic minerals such as pyrrhotite, pyrite, and arsenopyrite are also present and are distributed in a spotted pattern. The gangue minerals include calcite, biotite, chlorite, and epidote. Geochemical analysis of five samples has revealed that it has tungsten (W) contents of 4.85–10.1 ppm, molybdenum (Mo) contents of 0.67%–1.59%, copper (Cu) contents of 0.39%–1.00%, lead (Pb) contents of 19.4–758 ppm, and zinc (Zn) contents of 123–196 ppm.

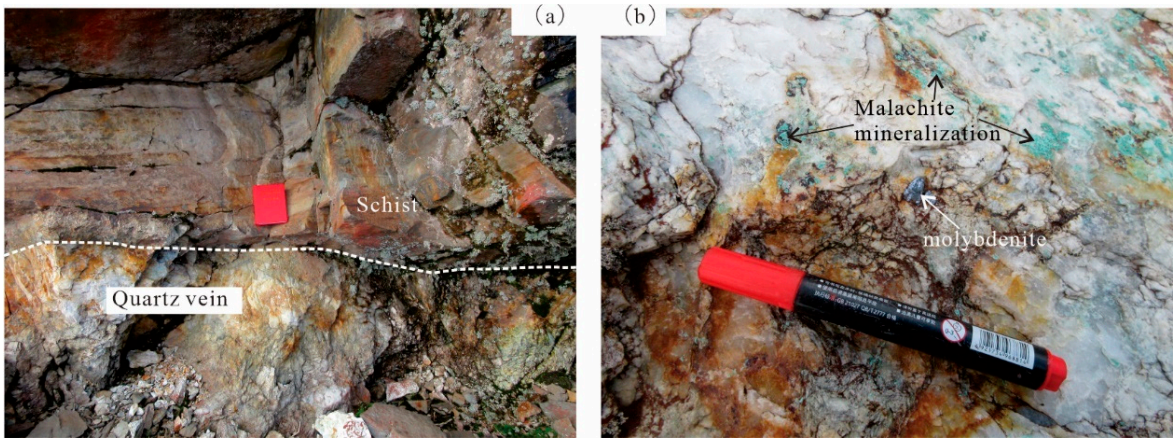

Figure 3. (a) Contact relationship between the Cu-Mo ore body and surrounding rock, and (b) distribution of molybdenite, malachite, and other minerals in quartz veins.

4. Sample Collection and Analytical Methods

4.1. Sample Collection and Description

The sampling locations and characteristics of the two molybdenite samples are shown in Figure 2. The main ore mineral in the deposit is molybdenite, minor associated minerals such as chalcocite, malachite, and chalcopyrite are also present, and the gangue main mineral is quartz. Molybdenite occurs in disseminated, flaky, and clustered forms on the surface of the quartz veins. It exhibits a flaky, bundled, and platy appearance, and there is local enrichment of molybdenite particles.

Sample T20200521-01 is a monzogranite (Figure 4a,b). It is grayish-white and has a fine-medium grained granitic texture and a massive structure. The rock is composed of plagioclase (25–40%), potassium feldspar (28–40%), quartz (25–32%), and biotite (3–7%), with minor titanite and hornblende. Sample T20200521-02 is a granitic pegmatite (Figure 4a), with grain sizes of 5–15 mm. Its primary mineral composition includes potassium feldspar (20%), plagioclase (40%), quartz (20%), biotite (5%), and muscovite (15%). Samples T20200521-03 and T20200521-04 are syenogranites (Figure 4b,d), which have a light gray color, fine-to-medium grained texture, and a massive structure. These rocks consist of plagioclase (10–12%), potassium feldspar (55%), quartz (25%), biotite (7%), and muscovite (1–3%). The plagioclase is primarily microcline, and under a microscope, albite and pericline twinning can be observed.

 doi:10.20944/preprints202408.0432.v1

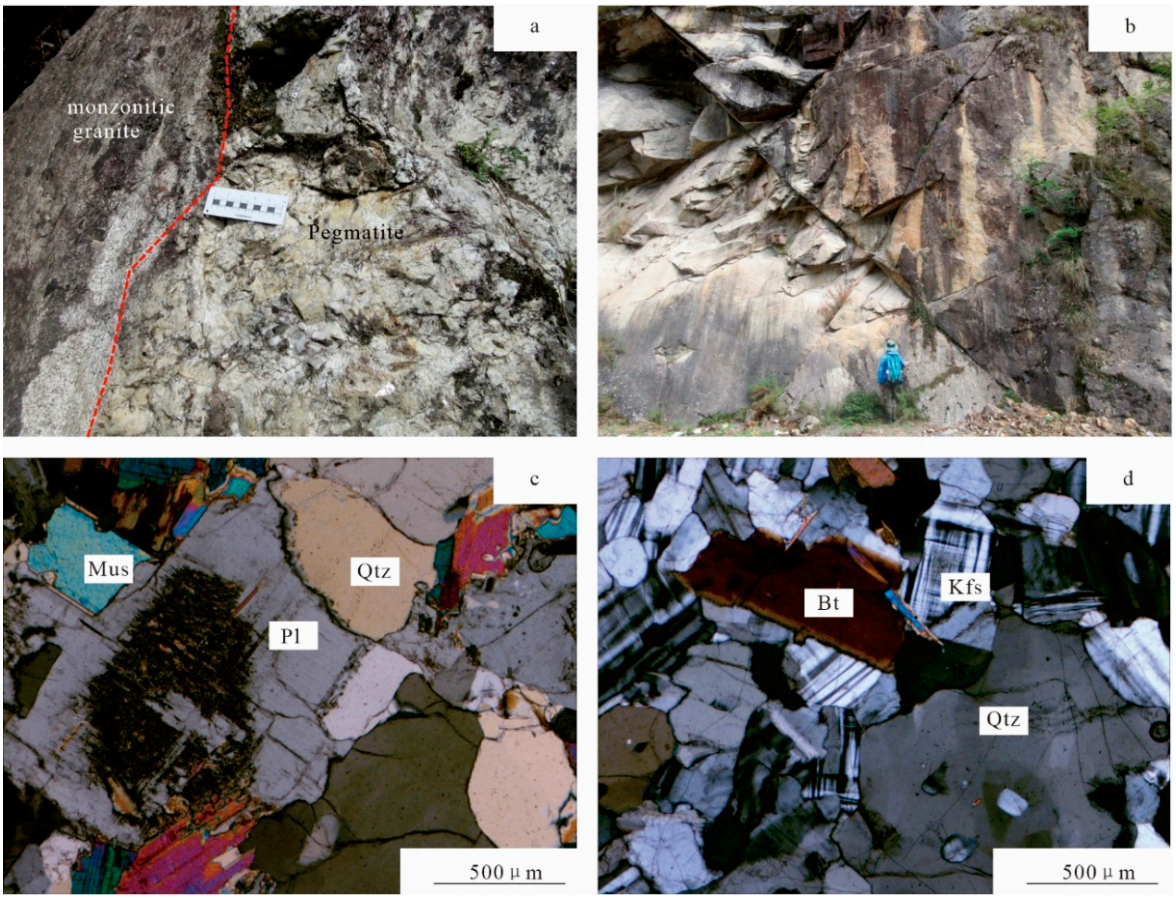

Figure 4. Microscopic characteristics of the (a,c) Tiechanghe monzonitic granite and (b,d) syenite granite in the Wulaxi area. Kfs—potassium feldspar, Mus—muscovite, BT—biotite, PL—plagioclase, QTZ—quartz. The images in c and d are all orthogonally polarized.

4.2. Analytical Methods

4.2.1. Zircon U-Pb Geochronology

Zircon grains were separated using standard heavy liquid and magnetic techniques, mounted in epoxy, and polished to expose the centers of the zircon grains. Cathodoluminescence (CL) images of the zircon grains were obtained, and the electron microprobe (JEOL JXA-8900RL) at Northwest University of China was used to examine the internal structures of the zircons. The U–Pb zircon dating was conducted via LA-MC-ICP-MS at the State Key Laboratory of the Continental Dynamics, Northwest University. The operating conditions for the laser ablation system and the multicoupled (MC)-ICP-MS instrument, as well as the data reduction, have been descried by Yuan et al. (2004) [51].

The laser ablation spot size was approximately 32 μm. The 207Pb/206Pb, 206Pb/238U, 237Pb/235U, and 208Pb/232Th ratios were calculated using GLITTER 4.0 (Macquarie University) and then were corrected using Harvard zircon 91500 as an external standard, which has a recommended 206 Pb/ 238U isotopic age of 1065.4 ± 0.6 Ma [52]. GJ-1 was also used as a standard sample, which has a recommended 206Pb/ 238U isotopic age of 603.2 ± 2.4 Ma. The details of the analytical techniques have been described by Yuan et al. (2004) [51]. The age calculations and plotting of the concordia diagrams were conducted using ISOPLOT (version 4.15) [53]. The uncertainties are quoted at the 2σ level.

4.2.2. Molybdenite Re-Os Isotope Dating

The samples were crushed, separated, and purified to obtain molybdenite with a purity >99%. Molybdenite Re-Os isotope analyses were carried out at the Re-Os Laboratory, National Research

 doi:10.20944/preprints202408.0432.v1

Center of Geoanalysis, Chinese Academy of Geological Sciences (CAGS, Beijing). The isotopic ratios of the molybdenite samples were analyzed using an inductively coupled plasma mass spectrometer (ICP-MS). Specifically, a JA X-series ICP-MS from TJA Inc was used. All of the molybdenite separated was prepared and analyzed using the procedures described by Du et al. (2004) [54].

5. Results

5.1. Zircon U-Pb Ages

In this study, we selected zircons from four samples (T20200521-01, T20200521-02, T20200521-03, and T20200521-04) of granite-pegmatite for U-Pb zircon isotopic measurement. The data are presented in Table 1, Figures 5 and 6.

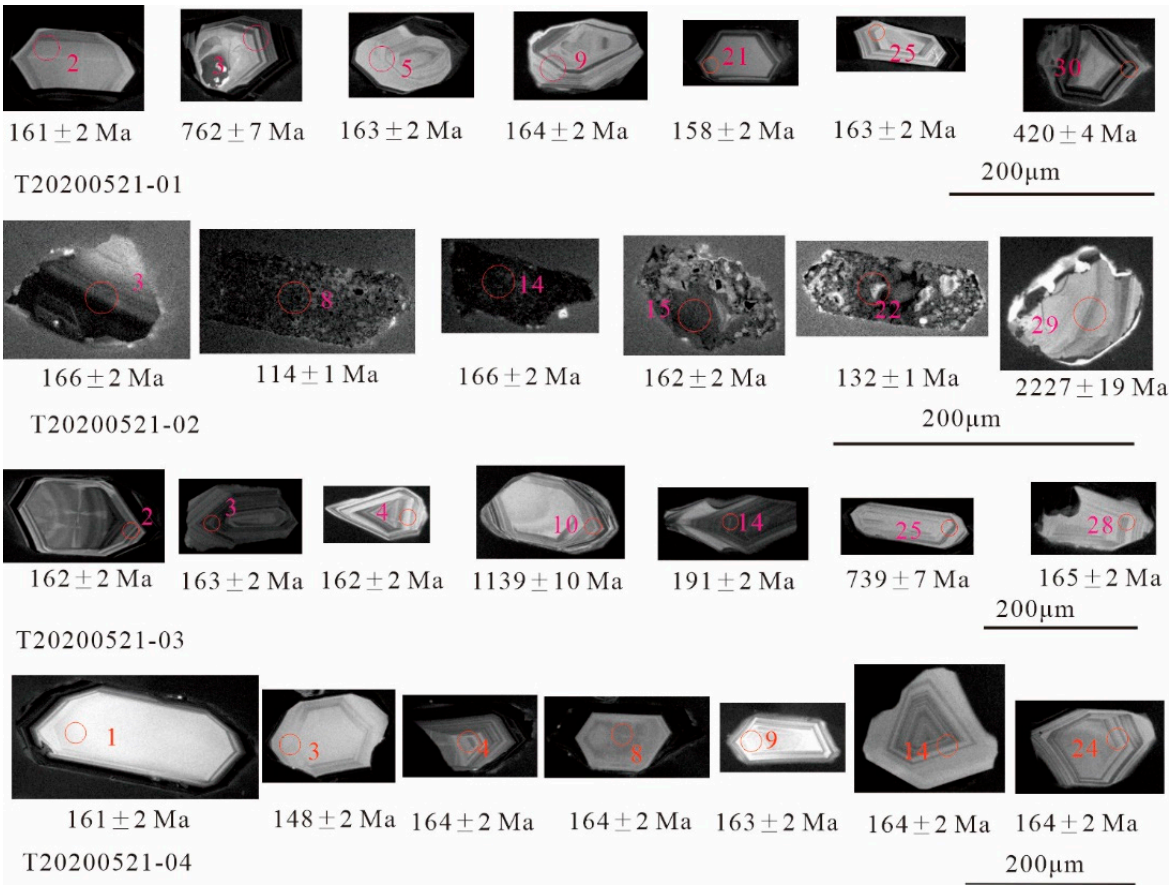

Figure 5. Cathode luminescence (CL) images of zircons from the Tiechanghe granite-pegmatite and corresponding U-Pb zircon ages.

Table 1. LA-ICP-MS zircon U-Pb isotopic age data of Tiechanghe granite-pegmatite.

Spot	Th ppm	U ppm	Th/U	Isotopic ratios						Age（Ma）						Concordant
				207Pb/206Pb	1σ	207Pb/235U	1σ	206Pb/238U	1σ	207Pb/206Pb	1σ	207Pb/235U	1σ	206Pb/238U	1σ	
T20200521-01																
1	240	339	0.71	0.04977	0.00143	0.17453	0.00392	0.02544	0.00027	184	66	163	3	162	2	99%
2	246	284	0.87	0.04958	0.00145	0.17322	0.00398	0.02534	0.00027	175	67	162	3	161	2	99%
3	111	219	0.51	0.06573	0.00153	1.13769	0.01728	0.12554	0.00128	798	48	771	8	762	7	99%
4	574	527	1.09	0.05034	0.00123	0.17674	0.00295	0.02546	0.00026	211	56	165	3	162	2	98%
5	145	244	0.59	0.05017	0.00137	0.17739	0.00364	0.02564	0.00027	203	62	166	3	163	2	98%
6	97	243	0.40	0.05178	0.00181	0.18337	0.00541	0.02568	0.00029	276	78	171	5	164	2	96%
7	69	279	0.25	0.04870	0.00155	0.17043	0.00442	0.02538	0.00028	133	73	160	4	162	2	101%
8	197	409	0.48	0.05120	0.00158	0.17934	0.00444	0.02540	0.00028	250	69	168	4	162	2	97%
9	88	340	0.26	0.04935	0.00133	0.17516	0.00350	0.02574	0.00026	164	62	164	3	164	2	100%
10	113	184	0.62	0.04949	0.00148	0.17574	0.00418	0.02575	0.00027	171	69	164	4	164	2	100%
11	91	226	0.40	0.07331	0.00154	1.73762	0.01924	0.17187	0.00166	1023	42	1023	7	1022	9	100%
12	100	283	0.35	0.04974	0.00133	0.17688	0.00347	0.02578	0.00026	183	61	165	3	164	2	99%
13	52	141	0.37	0.06084	0.00141	0.77701	0.01141	0.09259	0.00092	634	49	584	7	571	5	98%
14	355	496	0.72	0.04966	0.00119	0.17606	0.00278	0.02570	0.00025	179	55	165	2	164	2	99%
15	194	397	0.49	0.05027	0.00146	0.17944	0.00403	0.02587	0.00027	208	66	168	3	165	2	98%
16	156	232	0.67	0.05145	0.00151	0.18201	0.00418	0.02565	0.00027	261	66	170	4	163	2	96%
17	72	143	0.50	0.05006	0.00164	0.17724	0.00477	0.02567	0.00028	198	74	166	4	163	2	99%
18	108	226	0.48	0.05427	0.00176	0.19058	0.00505	0.02546	0.00028	382	71	177	4	162	2	91%
19	181	389	0.47	0.04877	0.00139	0.17060	0.00372	0.02536	0.00026	137	66	160	3	161	2	101%
20	78	1095	0.07	0.05132	0.00120	0.18216	0.00267	0.02573	0.00025	255	53	170	2	164	2	96%
21	154	327	0.47	0.05203	0.00195	0.17844	0.00576	0.02486	0.00029	287	83	167	5	158	2	95%
22	244	1355	0.18	0.05008	0.00108	0.17624	0.00208	0.02551	0.00024	199	49	165	2	162	2	99%
23	357	825	0.43	0.04888	0.00113	0.17156	0.00248	0.02544	0.00025	142	54	161	2	162	2	101%
24	93	325	0.28	0.05009	0.00131	0.17691	0.00331	0.02560	0.00026	199	60	165	3	163	2	98%
25	155	266	0.58	0.04976	0.00180	0.17587	0.00540	0.02562	0.00029	184	82	165	5	163	2	99%
26	84	1268	0.07	0.05513	0.00164	0.19507	0.00450	0.02564	0.00027	418	64	181	4	163	2	90%
27	99	2199	0.05	0.04856	0.00104	0.17230	0.00192	0.02572	0.00024	127	49	161	2	164	2	101%
28	204	893	0.23	0.04969	0.00115	0.17517	0.00248	0.02555	0.00025	180	53	164	2	163	2	99%
29	95	749	0.13	0.05159	0.00155	0.18178	0.00426	0.02554	0.00027	267	67	170	4	163	2	96%

doi:10.20944/preprints202408.0432.v1

30	133	999	0.13	0.05718	0.00123	0.53118	0.00601	0.06733	0.00064	498	47	433	4	420	4	97%
T20200521-02																
1	22	997	0.02	0.05225	0.00131	0.18429	0.00316	0.02558	0.00026	296	56	172	3	163	2	95%
2	77	3899	0.02	0.05385	0.00115	0.19398	0.00218	0.02612	0.00025	365	47	180	2	166	2	92%
3	84	6626	0.01	0.04968	0.00103	0.17845	0.00185	0.02605	0.00025	180	48	167	2	166	2	99%
4	111	5732	0.02	0.05273	0.00113	0.18748	0.00215	0.02578	0.00025	317	48	175	2	164	2	94%
5	78	3071	0.03	0.05062	0.00107	0.17905	0.00195	0.02565	0.00024	224	48	167	2	163	2	98%
6	195	4467	0.04	0.05160	0.00107	0.18513	0.00191	0.02602	0.00025	268	47	173	2	166	2	96%
7	2412	11496	0.21	0.05768	0.00120	0.20866	0.00220	0.02623	0.00025	518	45	192	2	167	2	87%
8	2174	27455	0.08	0.05087	0.00106	0.12539	0.00129	0.01788	0.00017	235	47	120	1	114	1	95%
9	622	9640	0.06	0.05681	0.00119	0.14045	0.00152	0.01793	0.00017	484	46	133	1	115	1	86%
10	151	4078	0.04	0.05090	0.00108	0.18200	0.00205	0.02593	0.00025	237	48	170	2	165	2	97%
11	1401	9235	0.15	0.05573	0.00123	0.19394	0.00245	0.02524	0.00024	441	48	180	2	161	2	89%
12	173	6260	0.03	0.05248	0.00115	0.16031	0.00198	0.02215	0.00021	306	49	151	2	141	1	94%
13	1770	35823	0.05	0.07937	0.00165	0.08525	0.00089	0.00779	0.00007	1181	41	83	1	50	0	60%
14	559	11465	0.05	0.05306	0.00109	0.19118	0.00192	0.02613	0.00025	331	46	178	2	166	2	94%
15	162	6370	0.03	0.05196	0.00113	0.18195	0.00226	0.02539	0.00025	283	49	170	2	162	2	95%
16	162	2600	0.06	0.05087	0.00112	0.18175	0.00233	0.02591	0.00025	235	50	170	2	165	2	97%
17	672	13506	0.05	0.04925	0.00108	0.17294	0.00219	0.02546	0.00025	160	51	162	2	162	2	100%
18	69	5088	0.01	0.05068	0.00113	0.17517	0.00233	0.02506	0.00024	226	51	164	2	160	2	97%
19	283	5187	0.05	0.05322	0.00110	0.19031	0.00197	0.02593	0.00025	338	46	177	2	165	2	93%
20	328	15458	0.02	0.05311	0.00109	0.19031	0.00194	0.02598	0.00025	334	46	177	2	165	2	93%
21	95	6872	0.01	0.05097	0.00108	0.14334	0.00160	0.02039	0.00020	239	48	136	1	130	1	96%
22	292	4453	0.07	0.05103	0.00107	0.14509	0.00158	0.02062	0.00020	242	48	138	1	132	1	96%
23	1295	13219	0.10	0.05847	0.00120	0.15799	0.00161	0.01959	0.00019	547	44	149	1	125	1	84%
24	215	7904	0.03	0.05014	0.00109	0.17634	0.00216	0.02550	0.00025	202	50	165	2	162	2	98%
25	127	4840	0.03	0.05075	0.00108	0.18221	0.00212	0.02603	0.00025	230	49	170	2	166	2	97%
26	2058	13841	0.15	0.05609	0.00118	0.12785	0.00143	0.01653	0.00016	456	46	122	1	106	1	86%
27	76	4336	0.02	0.05127	0.00113	0.18216	0.00234	0.02577	0.00025	253	50	170	2	164	2	97%
28	84	3293	0.03	0.05232	0.00110	0.18530	0.00205	0.02568	0.00025	300	47	173	2	164	2	95%
29	48	97	0.49	0.14065	0.00291	8.00227	0.08580	0.41257	0.00406	2235	35	2231	10	2227	19	100%
30	1154	30496	0.04	0.05101	0.00104	0.18113	0.00181	0.02575	0.00024	241	46	169	2	164	2	97%
T20200521-03																
1	164	276	0.59	0.04998	0.00139	0.17793	0.00372	0.02582	0.00027	194	63	166	3	164	2	99%

doi:10.20944/preprints202408.0432.v1

2	202	1102	0.18	0.04920	0.00135	0.17274	0.00353	0.02546	0.00026	158	63	162	3	162	2	100%
3	156	338	0.46	0.04970	0.00133	0.17512	0.00341	0.02555	0.00026	181	61	164	3	163	2	99%
4	254	625	0.41	0.04885	0.00117	0.17149	0.00268	0.02546	0.00025	141	55	161	2	162	2	101%
5	197	341	0.58	0.04988	0.00143	0.17734	0.00388	0.02579	0.00027	189	65	166	3	164	2	99%
6	124	175	0.71	0.04982	0.00167	0.17468	0.00485	0.02543	0.00028	187	76	164	4	162	2	99%
7	242	411	0.59	0.04937	0.00132	0.17597	0.00341	0.02585	0.00026	166	61	165	3	165	2	100%
8	231	881	0.26	0.04953	0.00137	0.17102	0.00355	0.02504	0.00026	173	63	160	3	160	2	100%
9	314	470	0.67	0.05040	0.00147	0.17865	0.00401	0.02571	0.00027	213	66	167	3	164	2	98%
10	191	466	0.41	0.07735	0.00161	2.06110	0.02129	0.19325	0.00185	1130	41	1136	7	1139	10	100%
11	201	328	0.61	0.05108	0.00168	0.18353	0.00497	0.02606	0.00029	244	74	171	4	166	2	97%
12	305	320	0.95	0.05213	0.00141	0.18294	0.00363	0.02545	0.00026	291	61	171	3	162	2	95%
13	100	210	0.48	0.04910	0.00147	0.17634	0.00417	0.02605	0.00027	153	69	165	4	166	2	100%
14	63	172	0.37	0.05063	0.00180	0.20958	0.00630	0.03002	0.00034	224	80	193	5	191	2	99%
15	191	419	0.46	0.05006	0.00138	0.17512	0.00357	0.02537	0.00026	198	63	164	3	162	2	99%
16	202	455	0.44	0.04991	0.00140	0.17704	0.00374	0.02572	0.00027	191	64	166	3	164	2	99%
17	78	268	0.29	0.05213	0.00144	0.18470	0.00378	0.02569	0.00027	291	62	172	3	164	2	95%
18	127	627	0.20	0.05004	0.00123	0.17404	0.00286	0.02522	0.00025	197	56	163	2	161	2	99%
19	167	1990	0.08	0.05234	0.00116	0.20104	0.00258	0.02786	0.00027	300	50	186	2	177	2	95%
20	305	348	0.88	0.05197	0.00152	0.18355	0.00416	0.02561	0.00027	284	66	171	4	163	2	95%
21	262	456	0.57	0.05010	0.00133	0.17781	0.00343	0.02573	0.00027	200	61	166	3	164	2	99%
22	211	1139	0.19	0.05053	0.00114	0.17972	0.00241	0.02579	0.00025	219	51	168	2	164	2	98%
23	158	655	0.24	0.05033	0.00119	0.17912	0.00269	0.02581	0.00026	210	54	167	2	164	2	98%
24	258	614	0.42	0.05038	0.00125	0.18030	0.00304	0.02595	0.00026	213	57	168	3	165	2	98%
25	272	245	1.11	0.06608	0.00147	1.10665	0.01439	0.12142	0.00121	809	46	757	7	739	7	98%
26	301	406	0.74	0.05116	0.00134	0.18032	0.00336	0.02555	0.00026	248	59	168	3	163	2	97%
27	68	719	0.10	0.05005	0.00156	0.17822	0.00444	0.02582	0.00028	197	71	167	4	164	2	99%
28	120	214	0.56	0.05009	0.00143	0.17875	0.00391	0.02587	0.00027	199	65	167	3	165	2	99%
29	259	404	0.64	0.04939	0.00129	0.17652	0.00328	0.02591	0.00027	166	60	165	3	165	2	100%
30	170	994	0.17	0.05087	0.00117	0.18085	0.00256	0.02577	0.00026	235	52	169	2	164	2	97%
T20200521-04																
1	132	208	0.64	0.05009	0.00223	0.17434	0.00699	0.02524	0.00032	199	100	163	6	161	2	98%
2	172	253	0.68	0.04810	0.00173	0.17302	0.00529	0.02608	0.00029	104	83	162	5	166	2	102%
3	102	186	0.55	0.04949	0.00152	0.15861	0.00388	0.02324	0.00025	171	70	150	3	148	2	99%
4	148	368	0.40	0.05063	0.00129	0.17996	0.00320	0.02577	0.00026	224	58	168	3	164	2	98%

doi:10.20944/preprints202408.0432.v1

5	195	398	0.49	0.04933	0.00127	0.17383	0.00316	0.02555	0.00026	164	59	163	3	163	2	100%
6	152	229	0.66	0.04986	0.00188	0.17445	0.00570	0.02537	0.00029	188	86	163	5	162	2	99%
7	254	488	0.52	0.05161	0.00131	0.18287	0.00321	0.02569	0.00026	268	57	171	3	164	2	96%
8	296	572	0.52	0.05031	0.00120	0.17845	0.00271	0.02571	0.00025	210	54	167	2	164	2	98%
9	471	990	0.48	0.04868	0.00124	0.17188	0.00303	0.02560	0.00026	133	59	161	3	163	2	101%
10	22	412	0.05	0.05073	0.00141	0.17891	0.00371	0.02557	0.00026	229	63	167	3	163	2	97%
11	84	1125	0.08	0.04942	0.00110	0.17501	0.00223	0.02567	0.00025	168	51	164	2	163	2	100%
12	316	2283	0.14	0.05010	0.00111	0.17832	0.00220	0.02581	0.00025	200	50	167	2	164	2	99%
13	197	311	0.63	0.04970	0.00198	0.17658	0.00614	0.02576	0.00031	181	90	165	5	164	2	99%
14	202	401	0.50	0.05023	0.00129	0.17808	0.00316	0.02571	0.00026	205	58	166	3	164	2	98%
15	238	395	0.60	0.05145	0.00137	0.18109	0.00344	0.02552	0.00026	261	60	169	3	162	2	96%
16	195	386	0.50	0.05217	0.00143	0.18472	0.00369	0.02567	0.00026	293	61	172	3	163	2	95%
17	184	310	0.59	0.04852	0.00133	0.17079	0.00341	0.02552	0.00026	125	63	160	3	162	2	101%
18	96	1029	0.09	0.05069	0.00114	0.17828	0.00230	0.02550	0.00024	227	51	167	2	162	2	97%
19	120	280	0.43	0.05125	0.00312	0.18847	0.01072	0.02666	0.00042	252	134	175	9	170	3	97%
20	88	592	0.15	0.05067	0.00128	0.18120	0.00309	0.02593	0.00026	226	57	169	3	165	2	98%
21	60	129	0.46	0.04975	0.00210	0.17657	0.00660	0.02573	0.00031	184	95	165	6	164	2	99%
22	179	252	0.71	0.05093	0.00163	0.17956	0.00463	0.02556	0.00027	238	72	168	4	163	2	97%
23	90	2728	0.03	0.05055	0.00118	0.17837	0.00251	0.02558	0.00025	221	53	167	2	163	2	98%
24	145	259	0.56	0.05107	0.00167	0.18135	0.00479	0.02575	0.00028	244	73	169	4	164	2	97%
25	118	190	0.62	0.05043	0.00183	0.17988	0.00551	0.02586	0.00029	215	82	168	5	165	2	98%
26	197	572	0.34	0.05143	0.00127	0.18148	0.00291	0.02559	0.00025	260	56	169	3	163	2	96%
27	131	268	0.49	0.04935	0.00177	0.17534	0.00531	0.02577	0.00029	164	82	164	5	164	2	100%
28	131	212	0.62	0.05122	0.00167	0.18115	0.00477	0.02565	0.00028	251	73	169	4	163	2	97%
29	112	434	0.26	0.05269	0.00161	0.18424	0.00439	0.02536	0.00027	315	68	172	4	161	2	94%
30	610	565	1.08	0.05008	0.00125	0.17464	0.00285	0.02529	0.00025	199	57	163	2	161	2	99%

doi:10.20944/preprints202408.0432.v1

 doi:10.20944/preprints202408.0432.v1

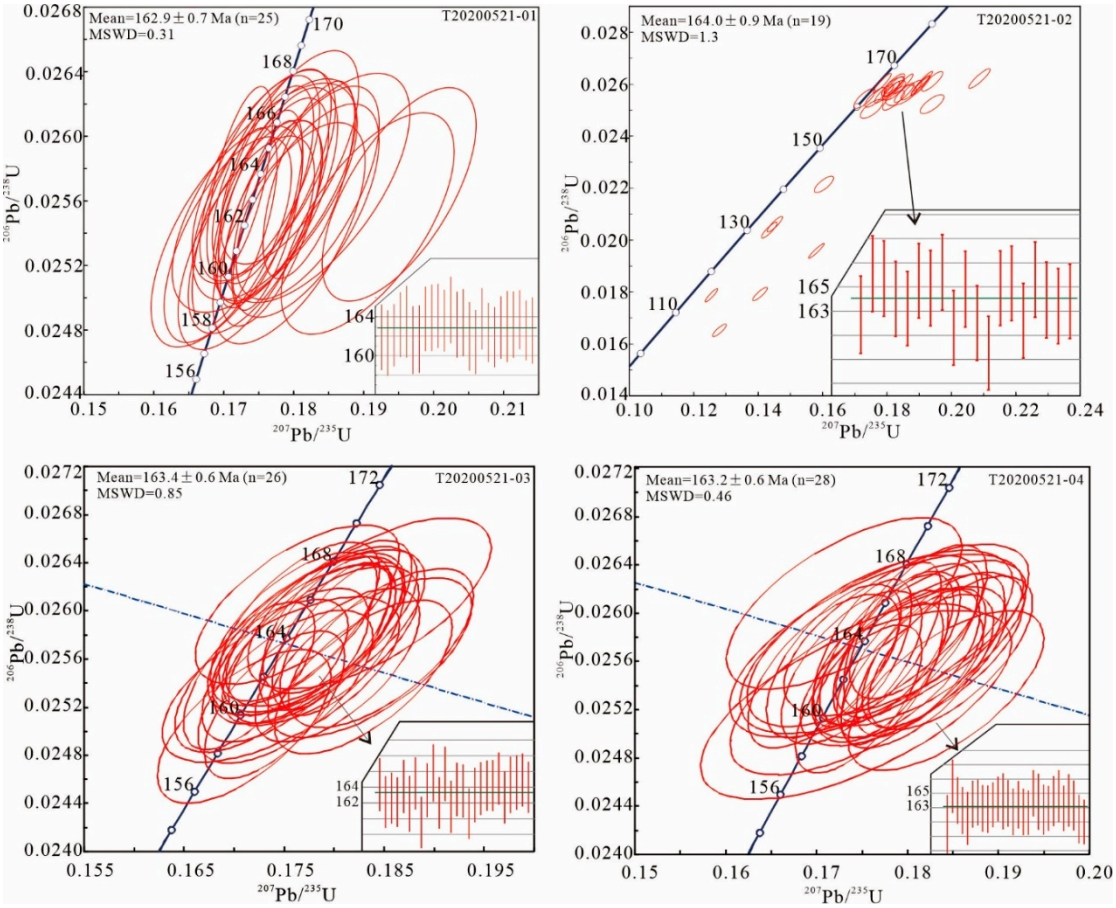

Figure 6. (a) U-Pb zircon concordia diagram and (b) weighted average ages of the Tiechanghe granite.

For sample T20200521-01, the zircons selected from the quartz monzonite are colorless and transparent, stubby to elongate prisms (120–300 μm long) with aspect ratios of 1:1–3:1 (Figure 5). In the CL images, most of the zircons exhibit well-defined oscillatory zoning, indicating a magmatic origin, and several zircons exhibit light cores, indicating that they are wall-rock xenocrysts or are inherited (Figure 5). Thirty spots were analyzed, and spots 3, 11, 13, and 30 have 206 Pb/ 238 U ages of 762 ± 7, 1022 ± 9, 571 ± 5, and 420 ± 4 Ma, respectively, which are the ages of the xenocrysts or zircons inherited from the surrounding strata (Table 1). The other 26 spots have concordant 206 Pb/ 238 U ages of 164–158 Ma, with a weighted mean age of 162.9 ± 0.7 Ma (MSWD = 0.31, n = 26), representing the peak crystallization age of the quartz monzonite. The age of 164 Ma is the starting crystallization time of magma, and the age of 158 Ma is the terminal crystallization time of magma. These zircons have variable Th contents of 69–574 ppm, U contents of 141–2199 ppm, and Th/U ratios of 0.05–1.09. Spot analyses of different zircon domains revealed that there is a significant difference in the rare earth element (REE) patterns (Figure 7). The spots on 26 zircons used in the age calculations exhibited HREE (158–1638 ppm) enrichment patterns and strongly negative Eu (Eu/Eu* = 0.03–0.32) and positive Ce (Ce/Ce* = 1.32–101) anomalies. The zircon Ti thermometer [55] yielded temperatures of 632 °C–784 °C (average 690 °C). The CL images and REE contents of the zircons confirm that the age of 162.9 ± 0.7 Ma represents the crystallization age of the quartz monzonite.

 doi:10.20944/preprints202408.0432.v1

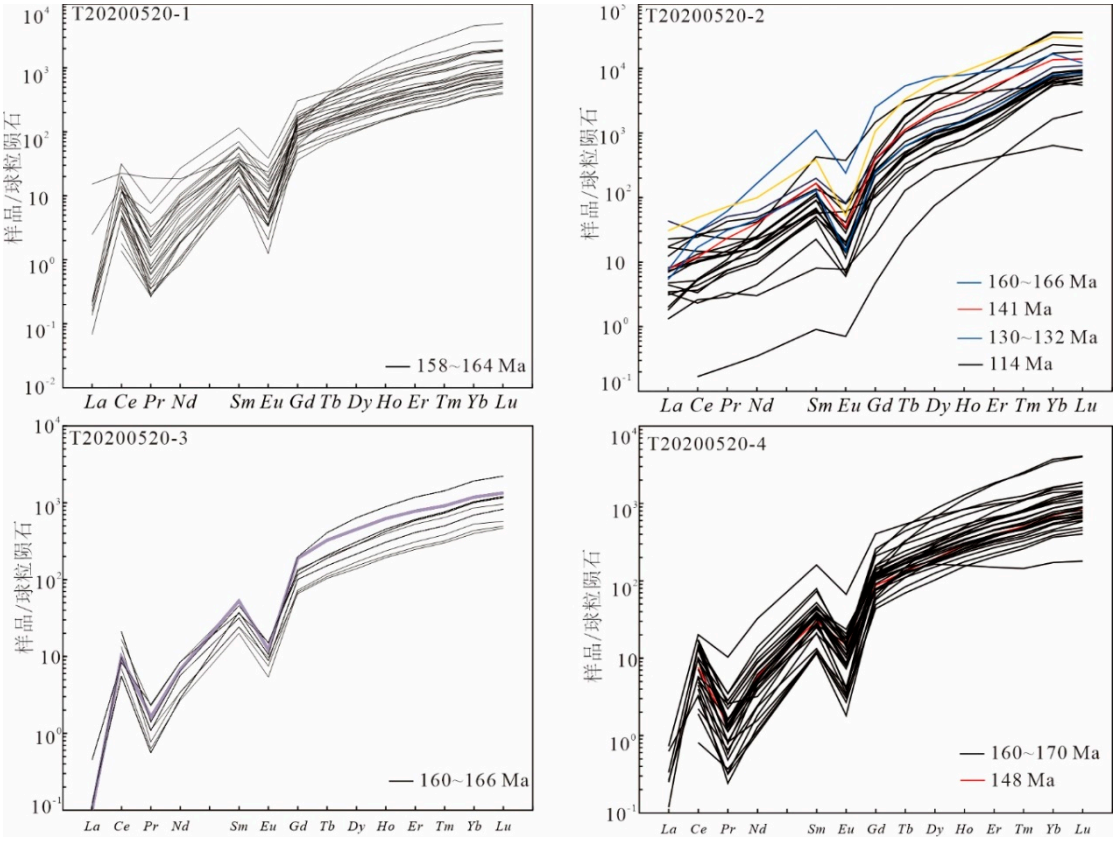

Figure 7. Standardized partition map of the rare-earth Chondrite patterns for the zircons from the Tiechanghe granite.

For sample T20200521-02, the zircons selected from the granite pegmatite are colorless and transparent, stubby to elongate prisms (140–340 μm long), with aspect ratios of 1:1–2:1 (Figure 5). In the CL images, most of the zircons exhibit well-defined oscillatory zoning, indicating that they have a magmatic origin, and several zircons exhibit light cores, are black, and have an irregular shape, indicating that they are wall-rock xenocrysts or are inherited and have experienced Pb loss (Figure 5). Thirty spots were analyzed, excluding six zircons with concordances <90% and one captured zircon (Table 1). Spots 8, 12, 21, and 22 have 206 Pb/ 238 U ages of 114 ± 1, 141 ± 1, 130 ± 1, and 132 ± 1 Ma, respectively, which represent the ages of tectonic thermal events (Table 1). The other 19 spots have concordant 206 Pb/238 U ages of 160–166 Ma, with a weighted mean age of 164.1 ± 0.9 Ma (MSWD = 1.3, n = 19), indicating that they represent the peak crystallization age of the granite pegmatite. The age of 166 Ma is the starting crystallization time of the magma, and the age of 160 Ma is the terminal crystallization time of the magma. These zircons have variable Th contents of 22–1154 ppm, U contents of 997–30496 ppm, and Th/U ratios of 0.01–0.06. The spot analyses on different zircon domains yielded significantly different REE patterns (Figure 7). The spots on 19 zircons included in the age calculations have HREE (300–11077 ppm) enrichment patterns and strongly negative Eu (Eu/Eu* = 0.06–0.76) and positive Ce (Ce/Ce* = 0.57–1.50) anomalies. The zircon Ti thermometer [55] yielded temperatures ranging from 578 °C to 838 °C (average of 681 °C). The CL images and REE contents of the zircons confirm that the age of 164.1 ± 0.9 Ma represents the crystallization age of the quartz monzonite. This age is consistent with the crystallization age of the monzogranite within the error range.

For sample T20200521-03, the zircons selected from the syenogranite are colorless, transparent, stubby to elongate prisms (140–300 μm long) with aspect ratios of 1:1–2:1 (Figure 5). In the CL images, most of the zircons exhibit well-defined oscillatory zoning, indicating that they have a magmatic origin, and several zircons have light cores, indicating that they are wall-rock xenocrysts or are inherited (Figure 5). Thirty spots were analyzed, and spots 14, 19, and 25 yielded 206 Pb/238 U ages

 doi:10.20944/preprints202408.0432.v1

of 191 ± 2, 177 ± 2, and 739 ± 7 Ma, respectively, and they represent the ages of the xenocrysts or inherited zircons from surrounding strata (Table 1). The other 26 spots have concordant 206 Pb/238 U ages of 166–160 Ma, with a weighted mean age of 163.4 ± 0.6 Ma (MSWD = 0.68, n = 26), and they represent the peak crystallization age of the syenogranite. The age of 166 Ma is the starting crystallization time of the magma, and the age of 160 Ma is the terminal crystallization time of the magma. These zircons have variable Th contents of 68–314 ppm, U contents of 175–1139 ppm, and Th/U ratios of 0.10–0.95. Spot analyses on different zircon domains revealed that they have significantly different REE patterns (Figure 7). The spots from 26 zircons involved in the age calculations have HREE (184–881 ppm) enrichment patterns and strong negative Eu (Eu/Eu* = 0.08–0.27) and positive Ce (Ce/Ce* = 1.49–34.87) anomalies. The zircon Ti thermometer [55] yielded temperatures ranging from 648 °C to 810 °C (average 714 °C). The CL images and REE contents of the zircons confirm that the age of 163.4 ± 0.6 Ma represents the crystallization age of the syenogranite.

For sample T20200521-04, the zircons selected from the syenogranite are colorless, transparent, stubby to elongate prisms (120–300 μm long), with aspect ratios of 1:1–3:1 (Figure 5). In the CL images, most of the zircons exhibit well-defined oscillatory zoning, indicating a magmatic origin, and several zircons have light cores, indicating that they are wall-rock xenocrysts or inherited zircons (Figure 5). Thirty spots were analyzed, and spot 3 had a 206 Pb/238 U age of 148 ± 2 Ma, which is the age of a tectonic-thermal event (Table 1). The other 29 spots yielded concordant 206 Pb/238 U ages of 161–170 Ma, with a weighted mean age of 163.2± 0.6 Ma (MSWD = 0.68, n = 29), representing the peak crystallization age of the syenogranite. The age of 170 Ma is the starting crystallization time of the magma, and the age of 161 Ma is the terminal crystallization time of the magma. These zircons have variable Th contents of 22–610 ppm, U contents of 129–2728 ppm, and Th/U ratios of 0.03–1.08. Spot analyses on different zircon domains yielded significantly different REE patterns (Figure 7). The spots from 29 zircons involved in the age calculations exhibited HREE (132–1408 ppm) enrichment patterns with strong negative Eu (Eu/Eu* = 0.04–0.29) and positive Ce (Ce/Ce* = 3.63–33.07) anomalies. The zircon Ti thermometer [55] yielded temperatures ranging from 614 °C to 768 °C (average 700 °C). The CL images and contents of the zircons confirm that the age of 163.2 ± 0.6 Ma represents the crystallization age of the syenogranite.

5.2. Re-Os Isotope Dating of Molybdenite

Re-Os data for two samples are presented in Table 2. The samples have moderate Re and Os concentrations (187Re concentration of 3.97–7.72 ppm, and 187Os concentration of 10.67–20.52 ppb) and model ages ranging from 161.1 ± 2.2 Ma to 159.4 ± 2.5 Ma, with an average of 160.3 ± 1.6 Ma (MSWD = 1.05).

Table 2. Zircon trace element data of Tiechanghe granite in Jiulong region.

Spot	Ti	La	Ce	Pr	Nd	Sm	Eu	Gd	Tb	Dy	Ho	Er	Tm	Yb	Lu	Y	ΣREE	L	H	L/H	δEu	δCe	T (℃)
	T20200521-01																						
1	5.99	<0.03	7.63	0.26	4.93	8.92	0.85	34.93	9.39	84.7	25.0	91.6	16.1	141.3	25.0	732	451	23	428	0.05	0.13	8.97	700
2	6.99	0.04	7.00	0.51	7.75	10.75	1.16	31.88	8.15	70.4	19.9	71.0	12.3	107.3	18.2	585	366	27	339	0.08	0.18	4.16	713
4	9.02	0.05	19.24	0.72	12.44	17.70	2.23	62.58	15.74	135.0	38.7	134.5	23.3	193.3	31.9	1122	687	52	635	0.08	0.18	8.11	736
5	7.14	<0.02	7.13	0.16	3.50	5.73	0.97	20.75	5.58	51.1	16.1	62.8	11.8	110.6	19.9	478	316	17	299	0.06	0.24	13.50	715
6	3.38	3.60	13.77	1.79	8.53	6.20	0.39	16.28	4.45	41.1	11.9	44.0	8.1	70.3	12.4	345	243	34	208	0.16	0.11	1.32	653
7	5.55	<0.03	2.51	0.03	0.48	1.64	0.20	7.39	2.50	25.7	8.6	36.1	7.5	71.1	13.1	279	177	5	172	0.03	0.15	27.83	693
8	6.28	<0.02	8.03	0.13	2.37	6.97	0.45	26.59	7.12	67.3	20.9	80.9	15.0	132.0	22.3	626	390	18	372	0.05	0.09	19.79	704
9	3.03	<0.02	8.10	0.02	0.84	2.68	0.32	13.90	5.08	53.4	17.1	67.4	12.8	119.7	20.8	513	322	12	310	0.04	0.13	100.99	645
10	5.90	<0.02	4.75	0.07	1.19	2.99	0.27	11.86	3.19	29.3	8.9	34.5	6.3	57.3	9.9	268	171	9	161	0.06	0.12	21.37	699
12	2.88	<0.03	2.90	0.05	0.89	2.10	0.19	11.14	3.64	36.7	12.0	46.3	8.9	81.6	14.2	351	221	6	214	0.03	0.10	19.83	641
14	6.16	0.05	12.37	0.22	3.97	8.54	1.11	37.14	10.66	102.1	31.0	120.1	22.1	197.1	33.1	948	579	26	553	0.05	0.16	16.20	702
15	7.66	0.59	8.60	0.31	3.53	5.16	0.47	25.36	7.16	70.1	21.9	81.8	15.4	136.3	22.0	648	399	19	380	0.05	0.10	4.91	721
16	7.11	0.05	4.79	0.19	2.99	5.22	0.66	19.02	5.25	47.2	14.6	56.5	10.4	96.4	15.9	438	279	14	265	0.05	0.18	7.18	715
17	4.20	<0.03	3.60	0.04	0.86	2.22	0.21	9.53	2.74	26.5	8.5	33.6	6.4	60.3	10.4	248	165	7	158	0.04	0.12	28.58	670
18	4.84	<0.03	4.18	0.11	1.62	4.26	0.50	17.53	4.79	45.2	13.7	52.2	10.0	90.1	15.0	409	259	11	248	0.04	0.15	12.02	682
19	6.90	<0.03	10.00	0.14	3.87	5.41	1.36	22.76	6.26	59.2	19.7	80.6	16.8	161.3	29.2	623	417	21	396	0.05	0.32	21.71	712
20	5.08	<0.02	1.11	0.03	0.87	4.51	0.26	30.66	12.11	130.1	41.7	162.7	32.0	304.3	48.9	1286	769	7	762	0.01	0.05	10.42	686
21	5.13	0.03	5.64	0.07	1.52	3.84	0.29	17.94	4.63	49.2	14.7	55.4	10.4	92.8	14.9	431	271	11	260	0.04	0.09	21.93	687
22	4.11	<0.034	3.66	0.06	1.15	4.34	0.20	33.09	13.34	155.5	54.7	225.0	46.0	424.1	67.1	1605	1028	9	1019	0.01	0.04	20.66	669
23	14.77	<0.025	10.23	0.22	4.56	8.53	1.61	41.23	12.11	121.8	40.1	157.7	31.0	285.5	48.0	1221	762	25	737	0.03	0.22	14.77	784
24	4.54	<0.0204	3.01	0.06	1.32	3.74	0.32	17.87	5.48	53.3	16.9	62.5	11.8	108.6	18.1	487	303	8	294	0.03	0.10	16.11	677
25	6.88	<0.019	7.63	0.15	2.64	4.83	0.76	21.31	5.64	55.2	17.8	68.0	13.4	122.9	21.1	531	341	16	325	0.05	0.19	15.90	712
26	3.11	<0.024	1.71	0.03	0.44	3.87	0.21	29.38	11.88	141.7	45.6	177.8	35.6	302.2	46.4	1426	797	6	791	0.01	0.04	20.42	647
27	2.56	<0.0262	0.84	0.03	0.51	2.41	0.12	24.42	13.42	194.5	77.4	355.4	79.1	768.9	125.0	2495	1642	4	1638	0.00	0.03	10.13	632
28	4.32	<0.028	5.39	0.08	2.08	5.05	0.67	26.60	9.17	103.3	35.0	142.9	29.5	280.0	45.4	1075	685	13	672	0.02	0.14	21.73	673
29	4.64	0.02	2.75	0.03	0.39	2.18	0.07	12.43	5.82	79.0	28.5	117.5	23.8	218.1	30.9	915	521	5	516	0.01	0.03	21.13	679
	T20200521-02																						
1	358.52	<0.026	0.10	<0.0125	0.16	0.14	0.04	0.97	0.89	19.1	9.4	58.6	20.2	281.6	54.4	367	446	0	445	0.00	0.25	1.39	1248
2	1.23	0.79	1.42	0.32	1.41	1.23	0.45	5.43	4.77	67.0	18.8	68.4	13.0	109.1	13.6	999	306	6	300	0.02	0.45	0.69	581
3	1.18	1.05	2.05	0.70	5.01	6.81	0.39	27.73	15.67	205.9	66.8	336.1	98.1	1203.4	200.0	2579	2170	16	2154	0.01	0.08	0.57	578

doi:10.20944/preprints202408.0432.v1

4	5.92	5.42	14.91	4.06	22.82	20.73	4.64	49.46	23.38	254.0	75.4	356.9	100.9	1277.3	219.3	2811	2429	73	2357	0.03	0.43	0.74	699
5	10.60	0.43	3.22	0.87	8.59	13.95	0.89	44.06	19.00	220.6	70.7	334.1	91.2	1114.9	199.5	2431	2122	28	2094	0.01	0.10	0.96	751
6	4.17	1.13	3.18	0.94	6.49	9.41	1.19	31.57	15.85	197.6	64.9	316.0	87.8	1041.7	178.1	2349	1956	22	1934	0.01	0.19	0.71	670
10	3.65	1.73	6.05	1.43	11.28	16.17	1.90	52.65	23.15	248.0	73.5	336.1	89.1	1046.9	180.1	2598	2088	39	2049	0.02	0.18	0.89	659
14	14.95	4.13	16.32	3.09	19.54	25.35	3.37	101.40	69.34	1036.2	358.4	1848.6	523.7	6224.1	915.5	13979	11149	72	11077	0.01	0.18	1.07	785
15	6.98	1.65	7.09	1.24	7.90	10.43	0.85	31.50	16.60	211.7	68.4	349.4	105.1	1338.6	223.0	2736	2373	29	2344	0.01	0.13	1.16	713
16	7.52	0.47	3.33	1.04	15.92	65.27	21.77	300.00	115.98	1036.0	234.0	737.2	127.3	1064.5	139.4	8195	3862	108	3754	0.03	0.40	0.84	720
17	24.65	10.28	17.88	4.81	28.36	30.37	4.76	79.12	38.49	421.2	119.0	529.3	145.0	1775.6	279.7	4450	3484	96	3387	0.03	0.28	0.62	838
18	1.42	0.31	1.59	0.27	2.04	3.46	0.35	13.94	8.79	123.8	46.4	259.5	83.8	1123.5	200.6	1705	1868	8	1860	0.00	0.13	1.25	591
19	5.69	1.84	8.12	1.68	11.64	17.62	1.63	66.71	38.64	507.8	163.5	816.4	231.1	2905.9	463.0	6364	5236	43	5193	0.01	0.13	1.04	696
20	17.84	1.94	6.15	1.23	8.03	13.63	2.38	87.26	65.46	1002.9	354.3	1829.0	501.3	5997.9	920.2	14014	10792	33	10758	0.00	0.16	0.95	803
24	1.88	0.74	2.68	0.72	4.92	7.82	0.81	31.00	17.74	248.8	91.3	462.5	124.6	1440.4	233.6	3366	2668	18	2650	0.01	0.14	0.82	610
25	1.28	1.37	6.45	1.25	11.00	17.76	0.67	53.84	27.35	304.6	87.5	408.5	115.3	1464.8	240.1	3289	2740	39	2702	0.01	0.06	1.11	584
27	2.50	0.82	2.24	0.63	4.40	7.48	1.17	22.70	12.27	151.3	46.6	232.2	70.0	911.2	155.3	1816	1618	17	1602	0.01	0.25	0.73	630
28	2.96	2.90	16.18	2.18	10.46	8.76	3.51	20.76	10.05	117.1	37.1	199.4	67.2	976.3	175.3	1392	1647	44	1603	0.03	0.76	1.50	643
30	6.51	4.01	9.00	1.35	7.57	10.01	1.05	62.07	50.69	786.2	271.4	1358.1	354.2	3966.6	559.6	10628	7442	33	7409	0.00	0.10	0.95	707
12	4.40	1.86	7.31	2.23	18.57	25.41	1.99	80.69	41.95	549.4	188.5	903.8	218.9	2322.5	355.3	6905	4718	57	4661	0.01	0.12	0.76	674
21	5.74	1.27	10.34	2.96	21.20	19.56	0.86	50.23	23.34	269.5	84.8	406.0	112.9	1343.0	213.5	3189	2559	56	2503	0.02	0.08	0.93	696
22	5.44	1.78	18.11	5.85	77.25	168.04	13.85	511.38	199.81	1866.2	447.8	1527.9	277.0	2832.8	308.6	17517	8257	285	7972	0.04	0.13	0.86	692
8	7.57	7.23	29.87	6.83	46.15	58.80	3.04	217.88	124.02	1606.0	507.0	2240.5	514.3	5199.1	739.3	18385	11300	152	11148	0.01	0.07	0.95	720
	T20200521-03																						
1	8.21	<0.027	12.64	0.25	4.39	8.03	1.04	25.24	6.41	56.8	16.9	67.4	12.9	116.5	21.8	531	350	26	324	0.08	0.20	15.63	728
2	5.16	0.03	3.40	0.05	1.32	5.72	0.62	40.47	15.27	161.2	50.1	195.3	36.4	325.9	56.2	1556	892	11	881	0.01	0.09	16.3337	687
3	5.16	<0.025	6.03	0.10	2.63	4.84	0.51	20.54	5.66	54.7	17.3	67.7	12.7	117.3	20.9	524	331	14	317	0.04	0.13	18.18	687
4	6.88	0.02	6.00	0.15	3.14	8.03	0.71	38.65	12.13	114.3	35.3	128.7	23.2	200.4	34.0	1046	605	18	587	0.03	0.10	11.38	712
5	19.04	0.11	5.14	0.23	3.96	5.56	0.88	23.77	7.09	71.2	24.0	96.9	18.6	170.5	29.6	743	457	16	442	0.04	0.20	5.96	810
6	6.26	<0.031	8.20	0.07	1.61	3.72	0.56	13.41	3.87	35.2	10.9	40.8	7.7	67.4	11.9	320	205	14	191	0.07	0.22	34.87	704
7	6.69	<0.029	12.92	0.13	3.01	7.03	0.87	26.53	7.75	78.6	25.6	99.9	19.3	174.6	30.7	774	487	24	463	0.05	0.17	29.93	709
8	6.62	<0.0215	7.07	0.09	1.74	5.93	0.53	30.00	10.01	105.9	34.8	134.9	25.1	224.4	36.1	1030	617	15	601	0.03	0.10	23.35	709
9	10.60	0.04	11.43	0.33	3.89	8.15	1.07	31.40	9.31	93.9	30.9	120.7	22.7	198.9	34.3	936	567	25	542	0.05	0.18	10.25	751
11	9.09	0.54	9.54	0.31	3.89	6.12	0.94	24.95	7.51	72.7	23.7	92.2	17.1	156.9	25.7	719	442	21	421	0.05	0.20	5.65	737
12	12.70	0.34	10.70	0.43	6.99	11.10	2.18	42.13	10.94	99.4	29.0	104.6	18.7	160.6	26.2	857	523	32	492	0.06	0.27	5.89	769
13	3.15	<0.039	4.26	0.06	1.25	3.05	0.31	14.13	4.06	38.3	11.5	43.6	8.1	73.7	12.5	342	215	9	206	0.04	0.12	22.04	648
15	12.00	0.02	6.23	0.25	4.26	8.72	0.90	33.68	9.58	94.5	30.9	128.1	24.5	219.0	37.5	951	598	20	578	0.04	0.14	7.58	763

doi:10.20944/preprints202408.0432.v1

16	6.95	<0.0250	6.30	0.12	2.66	5.44	0.88	22.28	6.68	70.1	23.8	95.7	19.0	177.8	31.2	706	462	15	447	0.03	0.21	15.77	713
17	4.46	<0.0237	2.62	0.06	0.70	2.23	0.23	12.18	3.89	35.8	10.4	38.3	7.3	65.1	10.7	308	189	6	184	0.03	0.11	14.79	675
18	6.15	0.03	2.37	0.11	1.78	5.48	0.51	29.24	9.55	93.8	29.7	113.1	22.3	201.0	34.8	883	544	10	533	0.02	0.10	6.08	702
20	9.40	7.29	25.93	2.49	18.25	12.98	1.91	42.81	11.81	105.1	31.1	115.4	20.4	183.2	29.3	921	608	69	539	0.13	0.22	1.49	740
21	7.51	<0.024	10.26	0.22	3.92	7.68	0.75	27.81	7.51	71.2	22.3	86.8	16.3	145.4	24.3	680	425	23	402	0.06	0.14	14.82	720
22	5.36	3.06	12.43	0.57	3.55	5.61	0.55	29.27	10.46	114.6	36.9	144.7	27.8	246.8	38.9	1115	675	26	649	0.04	0.11	2.14	691
23	5.52	0.03	3.51	0.17	3.01	7.44	0.69	36.89	11.68	107.6	31.5	111.4	20.2	179.3	29.1	929	543	15	528	0.03	0.10	5.98	693
24	6.18	<0.038	8.39	0.09	2.50	6.00	0.52	26.71	8.69	87.8	28.8	112.6	22.0	196.5	32.0	859	533	17	515	0.03	0.11	28.62	703
26		2.52	17.03	0.83	6.48	8.67	1.17	32.87	9.50	91.4	28.7	107.6	19.8	173.5	28.3	847	528	37	492	0.07	0.19	2.87	
27	3.21	<0.026	1.09	<0.0212	0.64	3.30	0.30	23.32	9.44	95.4	30.6	117.9	23.8	217.2	33.5	921	557	5	551	0.01	0.08	2.28	649
28	5.06	0.03	5.97	0.11	1.58	3.67	0.44	14.89	4.40	42.9	13.4	51.2	9.8	89.9	14.6	398	253	12	241	0.05	0.16	16.05	686
29	7.75	1.31	13.29	0.36	3.40	5.73	0.71	27.38	8.37	79.8	24.8	92.0	17.2	153.0	24.2	731	452	25	427	0.06	0.14	4.65	722
30	8.72	<0.028	3.98	0.17	2.99	7.48	0.82	40.42	13.30	130.4	41.4	163.3	32.1	305.2	51.1	1283	793	15	777	0.02	0.12	7.35	733
	T20200521-04																						
1	6.20	<0.045	5.74	0.08	2.42	5.18	0.46	18.33	4.59	43.1	13.1	48.8	9.1	77.7	14.9	385	243	14	230	0.06	0.13	23.76	703
2	6.12	0.03	8.72	0.11	2.80	5.90	0.88	24.51	6.44	62.6	19.3	74.4	13.5	124.1	22.2	579	365	18	347	0.05	0.19	22.71	702
3	12.55	<0.0224	4.64	0.13	2.73	4.62	0.85	17.81	4.97	48.9	16.5	66.0	12.8	118.4	21.9	497	320	13	307	0.04	0.25	11.43	768
4	2.93	<0.0225	2.99	0.11	1.92	4.34	0.24	18.77	5.53	53.9	16.6	64.0	12.0	109.4	19.7	487	309	10	300	0.03	0.07	8.76	642
5	5.73	<0.035	8.63	0.16	2.49	5.43	0.49	24.29	7.19	68.9	21.8	86.4	16.2	147.6	26.2	675	416	17	399	0.04	0.11	17.29	696
6	6.12	<0.028	7.95	0.16	2.14	5.49	0.74	20.86	5.46	46.7	14.6	55.5	10.4	93.5	16.9	433	280	16	264	0.06	0.18	15.92	702
7	8.51	0.06	6.19	0.27	4.56	7.97	1.09	32.23	9.09	85.3	27.2	105.9	20.7	189.4	35.1	819	525	20	505	0.04	0.18	6.57	731
8	4.17	<0.036	7.68	0.33	6.51	12.09	0.81	42.89	11.26	102.6	30.3	110.4	19.7	169.8	28.1	872	542	27	515	0.05	0.10	7.14	670
9	7.59	0.08	8.81	0.33	5.41	11.13	0.93	53.25	16.45	158.3	47.8	178.8	31.9	274.9	47.5	1413	836	27	809	0.03	0.10	7.58	721
10	4.45	<0.034	0.50	0.04	0.53	1.84	0.18	13.97	4.93	41.6	8.9	24.7	3.7	29.3	4.6	277	135	3	132	0.02	0.08	4.39	675
11	2.76	0.15	2.01	0.08	0.73	1.77	0.11	12.29	5.58	74.2	28.4	129.5	27.7	268.9	47.4	896	599	5	594	0.01	0.05	4.54	638
12	6.76	<0.034	3.24	0.15	2.29	7.07	0.85	46.42	18.97	213.9	72.9	303.7	61.5	588.1	102.3	2291	1421	14	1408	0.01	0.11	6.75	710
13	9.14	<0.0278	10.31	0.13	2.40	6.00	1.03	26.10	7.07	70.5	23.1	87.8	16.6	147.8	26.5	693	425	20	405	0.05	0.21	25.61	738
14	7.69	<0.026	7.95	0.12	2.88	5.36	0.64	22.21	6.29	67.2	23.6	101.8	21.0	201.6	36.8	714	497	17	480	0.04	0.15	20.07	722
15	11.11	<0.023	10.54	0.24	4.04	7.22	0.94	28.05	7.93	80.3	26.7	106.2	20.1	177.0	31.1	810	500	23	477	0.05	0.18	13.75	756
16	6.25	<0.038	8.36	0.15	3.25	5.86	0.65	23.59	6.35	59.9	19.0	75.6	14.4	132.2	22.9	570	372	18	354	0.05	0.15	17.42	704
17	6.40	<0.0237	7.98	0.13	2.57	5.62	0.50	22.55	6.19	57.4	17.5	64.9	11.6	103.9	17.1	518	318	17	301	0.06	0.12	18.63	706
18	5.44	<0.0186	1.35	0.06	1.13	4.86	0.23	32.08	12.37	129.3	39.7	152.3	28.6	253.9	42.5	1225	698	8	691	0.01	0.04	6.77	692
19	3.17	0.06	3.52	0.25	1.49	3.88	0.42	15.87	4.57	45.7	13.8	52.0	9.7	90.4	15.2	412	257	10	247	0.04	0.14	4.05	648
20	3.52	<0.038	1.91	0.03	0.49	1.76	0.24	11.65	4.13	46.2	14.9	60.5	12.5	120.7	22.2	470	297	4	293	0.02	0.12	19.73	656

doi:10.20944/preprints202408.0432.v1

21	5.58	<0.034	2.74	0.05	1.10	2.03	0.19	8.93	2.60	25.9	8.7	33.7	6.6	62.1	10.2	254	165	6	159	0.04	0.12	18.49	694
22	6.86	<0.049	10.54	0.24	4.15	6.48	1.36	25.02	6.82	63.5	19.6	73.6	13.8	124.4	20.7	585	370	23	347	0.07	0.29	13.69	712
23	3.54	<0.0176	1.16	0.03	0.85	3.25	0.20	24.24	12.03	167.2	64.7	292.9	64.3	631.3	104.1	2049	1366	5	1361	0.00	0.05	11.66	657
24	8.24	<0.031	5.81	0.13	2.49	5.37	0.58	21.90	5.56	54.1	16.9	66.0	12.2	112.4	19.0	505	322	14	308	0.05	0.14	13.66	728
25	6.01	<0.029	9.23	0.12	2.14	4.11	0.90	16.20	4.67	44.6	13.8	54.3	10.4	94.2	16.4	419	271	16	254	0.06	0.29	23.88	700
26	7.47	<0.030	5.65	0.21	3.42	6.71	1.20	29.77	7.95	76.5	24.1	99.1	19.7	188.3	33.8	756	496	17	479	0.04	0.22	8.31	719
27	7.48	<0.027	3.44	0.06	2.16	3.14	0.50	15.71	5.12	48.5	15.8	61.8	11.9	105.9	18.0	467	292	9	283	0.03	0.18	19.42	719
28	7.83	<0.034	4.39	0.08	1.80	3.81	0.46	15.48	4.14	38.3	11.6	44.3	8.3	73.8	12.4	342	219	11	208	0.05	0.16	17.04	723
29	1.98	<0.030	2.45	0.02	0.60	1.88	0.16	10.05	3.12	31.8	10.0	37.5	7.3	65.7	11.5	291	182	5	177	0.03	0.09	33.07	614
30	10.27	0.17	12.27	0.98	15.10	24.44	3.86	82.89	20.18	173.6	47.5	162.3	28.1	235.2	36.7	1355	843	57	786	0.07	0.24	3.63	748

doi:10.20944/preprints202408.0432.v1

 doi:10.20944/preprints202408.0432.v1

6. Discussion

6.1. Implications of Zircon U-Pb and Molybdenite Re-Os Ages

Accurate dating of mineral deposits is fundamental for developing deposit models and interpreting the geodynamic background of the mineralization. It is crucial for understanding the formation processes of deposits, determining their genesis, exploring the coupling relationships between mineralization events and other geological events, and establishing mineralization and exploration models [56,57]. The reported crystallization ages of granitoids in the Songpan-Ganzi region predominantly range from 220 to 205 Ma, and most are I-type and S-type granitoids [13–17,20–22]. Only the Nianbaoyuze area has been reported to contain A-type granitoids [7]. A smaller group of granitoids have ages ranging from 165 to 150 Ma [31–34]. In the Jiulong area, the granitoids are primarily clustered into two age groups: 170–150 Ma and 220–200 Ma (Table 4), indicating that this region experienced two distinct magmatic events.

Table 3. Re-Os isotope data for molybdenite from the Ziershi W-Mo deposit in Jiulong region.

Sample	Weight (g)	Re (ppm)	2σ	Os (ppm)	2σ	187Re (ppb)	2σ	187Os (ppb)	2σ	Model age (Ma)	2σ
Z01	0.02	6.32	0.04	0.048	0.021	3.97	0.027	10.67	0.07	161.1	2.2
Z02	0.05	12.28	0.12	0.080	0.009	7.716	0.072	20.52	0.16	159.4	2.5

Table 4. The isotope chronology data of Tiechanghe area，west Sichuan.

No.	Unit	Location	Rock	Mineral	Method	genetic type	Age (Ma)	Reference
1	Sanyanlong-Fangmaping -Galazi	Sanyanlong-Fangmaping	Biotite monzonitic granite	Zircon	LA-ICP-MS	Adakite	208 ± 2	45
			Granodiorite	Zircon		I-type granite	212 ± 2	45
		Galazi	Monzonitic granite	Zircon	LA-ICP-MS	I-type granite	211.5 ± 1.2	17
			Granodiorite	Zircon	LA-ICP-MS	I-type granite	215.6 ± 1.1	17
2	Dingtianzhu	Dingtianzhu	Quartz monzonite	Zircon	LA-ICP-MS	I-type granite	228 ± 4	10
3	Riluku		porphyritic granite	Zircon	LA-ICP-MS	high K adakite	219 ± 6	10
			Biotite monzogranite	Zircon	LA-ICP-MS		207 ± 1	22
			Biotite monzogranite	Zircon	LA-ICP-MS		207 ± 1	22
			Biotite monzogranite	Zircon	LA-ICP-MS		206 ± 1	22
			Biotite monzogranite	Zircon	LA-ICP-MS		208 ± 1	22
			Biotite monzogranite	Zircon	LA-ICP-MS		207 ± 1	22
4	Lanniba	Lanniba	Biotite Granite	Zircon	LA-ICP-MS	I-type granite	211.4 ±1.5	44
			Muscovite syenite granite	Zircon	LA-ICP-MS	I-type granite	208.2 ± 1.6	38
			Biotite syenite granite	Zircon	LA-ICP-MS	I-type granite	173.5 ± 1.3	38
			Monzonitic granite	Zircon	LA-ICP-MS	I-type granite	208.3 ± 2.2	38
			Granodiorite	Zircon	LA-ICP-MS	I-type granite	214.6 ± 2.0	38
			Granodiorite	Zircon	LA-ICP-MS	I-type granite	216.5 ± 1.9	38
			Quartz diorite	Zircon	LA-ICP-MS	I-type granite	213.3 ± 1.8	38
6	Dichishan	Dichishan	Granite	Zircon	LA-ICP-MS	S-type granite	201.9 ± 0.8	25
			Pegmatite	molybdenite	Re-Os		188.6 ± 4.8	25
7	Yangfanggou	Yangfanggou	Syenite	Zircon	LA-ICP-MS	I-type granite	211.4 ± 1.5	10
8	Xinhuoshan	Xinhuoshan	Biotite Granite	Zircon	LA-ICP-MS	A-type granite	161.5 ± 0.6	29
		Daheibian south	Granite	Zircon	SHRIMP	——	176 ± 7	28
		Wenjiaping	Biotite Granite	Zircon	LA-ICP-MS		164.6 ± 0.9	33

 doi:10.20944/preprints202408.0432.v1

		Xinhuoshan	Biotite Granite	Zircon	LA-ICP-MS		161.5 ± 0.6	29
		Wenjiaping	Biotite Granite	Zircon	LA-ICP-MS		160.9 ± 1.0	48
		Wenjiaping	porphyraceous granite	Zircon	LA-ICP-MS		159.0 ± 0.7	34
		Xinhuoshan	Granite	Zircon	LA-ICP-MS	I-type granite	161.8 ± 1.2	62
		Xinhuoshan	Granite	Zircon	LA-ICP-MS	I-type granite	161.8 ± 1.7	62
		Xinhuoshan	Granite	Zircon	LA-ICP-MS	I-type granite	165.2 ± 1.1	62
		Xinhuoshan	Granite	Zircon	LA-ICP-MS	I-type granite	165.2 ± 1.4	62
		Shimenkan	Granite	Zircon	LA-ICP-MS		163.3 ± 0.7 154.5 ± 2.4 147.3 ± 2.3	34 34 34
		Shimenkan	Granite	Sphene	LA-ICP-MS		164.0 ± 3.0	34
		Shimenkan	Granite	Sphene	LA-ICP-MS		172.5 ± 1.9	34
		Shimenkan	Granite	Sphene	LA-ICP-MS		182.7 ± 2.5	34
		Shimenkan	Granite	Sphene	LA-ICP-MS		193.3 ± 3.6	34
		Shimenkan	Granite	Sphene	LA-ICP-MS		203.6 ± 2.9	34
		Xinhuoshan	Granite	Apatite	LA-ICP-MS		155.0 ± 4.8	34
9		Western and eastern Jiulong County	Granodiorite	Zircon	LA-ICP-MS		213 ± 1	22
			Monzonitic granite	Zircon	LA-ICP-MS		191 ± 1	22
10		Northern Jiulong County	Monzogabbro	Zircon	LA-ICP-MS		211 ± 1、217 ± 1	22
			Quartz monzonite	Zircon	LA-ICP-MS		208 ± 1	22
11	Wulaxi	Wulaxi	Two-mica granite	Zircon	LA-ICP-MS	A-type granite	159.3 ± 0.9	30
		Wulaxi	Two-mica granite	Zircon	SHRIMP		166.6 ± 1.1	50
		Wulaxi	Tungsten-molybdenum ore	Molybdenite	Re-Os		168.1 ± 6.4	60
		Wulaxi	Two-mica granite	Zircon	LA-ICP-MS		159.3 ± 0.9	30
		Wulaxi	Tungsten-molybdenum ore	Molybdenite	Re-Os		171.4 ± 1.7	34
		Wulaxi	Tungsten-molybdenum ore	Molybdenite	Re-Os		166.8 ± 1.7	35
		Zier	Tungsten-molybdenum ore	Molybdenite	Re-Os		160.3 ± 1.6	This paper
		Wulaxi	Granite	Zircon	LA-ICP-MS		166.0 ± 0.9	35
		Wulaxi	Granite	Zircon	LA-ICP-MS		158.9 ± 0.7	34
		Wulaxi	Granite	Zircon	LA-ICP-MS		163.1 ± 1.3 151.1 ± 1.8	34 34
		Wulaxi	Granite	Apatite	LA-ICP-MS		152.1 ± 4.6	34
		Wulaxi	Granite	Apatite	LA-ICP-MS		168.0 ± 4.6	34
		Wulaxi	Granite	Apatite	LA-ICP-MS		163.3 ± 1.7	34
		Wulaxi		Molybdenite	Re-Os		163.7 ± 1.9	50
		Wulaxi	Granite	Zircon	LA-ICP-MS	I-type granite	168.5 ± 1.1	62
		Wulaxi	Granite	Zircon	LA-ICP-MS	I-type granite	168.4 ± 1.2	62
		Wulaxi	Granite	Zircon	LA-ICP-MS	I-type granite	170.1 ± 0.5	62
		Wulaxi	Granite	Zircon	LA-ICP-MS	I-type granite	170.1 ± 0.6	62
		Wulaxi	Granite	Monazite	LA-ICP-MS		154.1 ± 0.7	34
12	Qiapengzi	Landiao	Monzonitic granite	Zircon	LA-ICP-MS		143.5 ± 1.0	26
			Monzonitic granite	Zircon	LA-ICP-MS		157.1 ± 1.6	26
		Qiaopengzi	Monzonitic granite	Zircon	LA-ICP-MS		147 ± 2	26
			Monzonitic granite	Zircon	LA-ICP-MS		168.2 ± 0.9	26
		Landiao	Monzonitic granite	Monazite	LA-ICP-MS		154.6 ± 0.6	26
		Landiao	Monzonitic granite	Monazite	LA-ICP-MS		152.8 ± 0.5	26
14	Baitai	Baitai	pegmatite	Columbite-tantalite	LA-ICP-MS		188.9 ± 1.6	24
			Biotite monzogranite	Zircon	LA-ICP-MS		212.6 ± 3.3	27
			Biotite monzogranite	Zircon	LA-ICP-MS		213.5 ± 1.7	27

 doi:10.20944/preprints202408.0432.v1

	Biotite monzogranite	Zircon	LA-ICP-MS		212.6 ± 1.8	27

The 220–200 Ma ages of the granitoids indicate that their formation was related to the magmatic activity triggered by the westward subduction and collision of the Ganzi-Litang Ocean during the Indosinian. This is consistent with previous studies that have suggested that the peak age of the closure of the Ganzi-Litang Ocean and the associated magmatic activity is around 216 Ma [55,56]. The 170–150 Ma granitoids reflect the Early Yanshanian magmatic events or tectonic thermal events in the Jiulong area, and their formation was related to post-collision extensional processes. Notably, this period also marks the stabilization of the neighboring Jianglang Dome [30,34].

The LA-ICP-MS U-Pb zircon ages of the Tiechanghe granite studied in this paper range from 162.9 ± 0.7 Ma to 163.4 ± 0.6 Ma. These results are consistent with previously reported zircon U-Pb ages for this region and represent the crystallization age of the Tiechanghe granite. The weighted average Re-Os age of the molybdenite is 160.3 ± 1.6 Ma, which is also consistent with earlier reported Re-Os isotope ages for this region, indicating that this is the molybdenum mineralization age in the Jiulong area. Additionally, the LA-ICP-MS U-Pb zircon ages of the granitic pegmatites (114 ± 1, 141 ± 1, 130 ± 1, and 132 ± 1 Ma) suggest that these zircons may have been influenced by later magmatic or tectonic thermal events or possibly by the loss of Pb.

The Sm-Nd isochron age of the Xuebaoding tungsten deposit in the northern edge of the Songpan-Ganzi Block is 182.0 ± 9.2 Ma [58,59]. The Re-Os isotope age of the molybdenite in the Hede tungsten-tin deposit in the Kangding region is 199.0 ± 2.6 Ma [39], while the Re-Os isotopic age of the molybdenite in the Daniuchang molybdenum-tungsten deposit is 166.8 ± 1.7 Ma [35]. The weighted average Re-Os age of the molybdenite in the Ziershi deposit is 160.3 ± 1.6 Ma, which is consistent with the LA-ICP-MS U-Pb zircon ages of the Tiechanghe granite (162–166 Ma) within the error margins. These ages collectively confirm that the molybdenite in the Ziershi deposit formed during the Early Yanshanian and that their formation was associated with granitic magmatism. These ages are consistent with those of the Daniuchang molybdenum-tungsten deposit within error [31,60], but they differ from those of the Xuebaoding W-Sn-Be deposit and the Hedong tungsten-tin deposit. This discrepancy suggests that significant magmatic activity related to Mo mineralization occurred in the Jiulong area at ca.166 Ma.

The geological and mineralization events in the Jiulong Tiechanghe region occurred approximately 40 Ma after the crustal collision and thickening event in the Songpan-Ganzi Block during 220-205 Ma. This period represents the peak of the lithospheric extension along the southern margin of the Songpan-Ganzi Block and marks the beginning of the thermal uplift and extension of the lithospheric after the contractional thrusting and detachment (collision orogeny) associated with the Songpan-Ganzi orogenic belt [29,60]. Consequently, the Tiechanghe granite is a product of the transition from compressional to extensional tectonic environments in the Songpan-Ganzi Block from the Indosinian to the Early Yanshanian. It is also a crucial time marker of the regional transition from the Tethyan tectonic domain to the Pacific tectonic domain.

6.2. Ore Formation Models and Geological Exploration Directions

The Daniuchang tungsten-molybdenum deposit is spatially closely associated with the Tiechanghe granite, which primarily consists of syenite and monzonitic granite. Zhou et al. (2014) reported that the Tiechanghe granite exhibits the characteristics of an aluminum-rich A-type granite, including high SiO_2, Na_2O, and K_2O contents, high FeO_o/MgO and Ga/Al ratios, and low TiO2, CaO, and MgO contents [30]. However, Liu Xiaojia and Xu Zhiqin (2021) argued that the Tiechanghe granite should be classified as a high-potassium calc-alkaline I-type granite [61]. This classification reflects the transition from collision orogeny to post-collisional extension, where decreased crustal stress led to partial melting of the ancient crust and contamination by newly formed crustal melts, resulting in Middle Jurassic magmatism. This perspective is consistent with the views of Dai et al. (2017) and Liu et al. (2022) [32,36].

The zircon Ti thermometer [63] can be used to infer the formation temperature of zircons, which represents the maximum temperature of the magma. Experimental petrology has revealed that A-

 doi:10.20944/preprints202408.0432.v1

type granites typically form at temperatures >800 °C. In contrast, the Ti thermometer calculations for the zircons analyzed in this study yielded temperatures of 690–714 °C. Therefore, based on the magma temperature, the Tiechanghe granite may not be an A-type granite but rather an I-type granite.

The Yanshanian granites, such as the Tiechanghe granite, which were formed in an extensional tectonic setting, provided the material and dynamic conditions necessary for the formation of tungsten-molybdenum-copper deposits due to multiple phases of granitoid magmatic activity. The Tiechanghe granite, characterized by high concentrations of mineralizing elements such as molybdenum (Mo), served as the primary mineralizing body in the region, and it supplied both the heat and material sources essential for the formation of the molybdenum deposits. During the Yanshanian, the intrusion of the Tiechanghe granite into the surrounding strata induced thermal contact metamorphism and metasomatism, resulting in the formation of skarns at the contact interfaces. The Triassic strata provided calcium, while the granite supplied tungsten and molybdenum, leading to the formation of scheelite and molybdenite in or near the skarn zone and thus creating the Daniuchang skarn-type W-Mo deposit. Additionally, in the schist areas located 2-3 km from the granite, quartz vein-type molybdenum deposits were more likely to form (Figure 8).

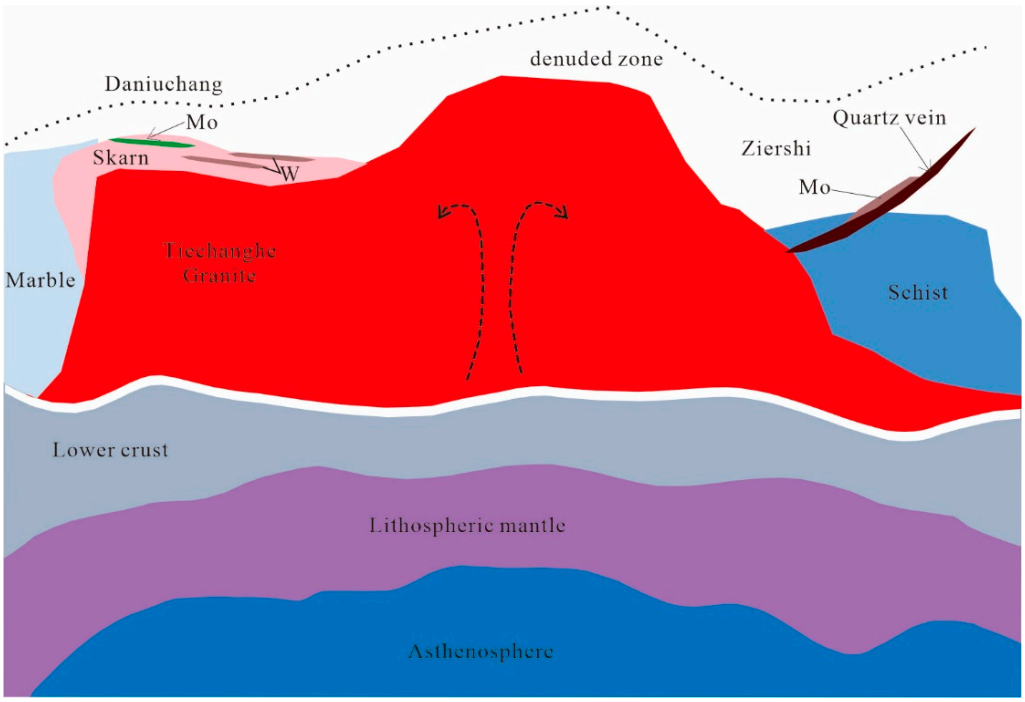

Figure 8. Map of molybdenum metallogenic model for the west Sichuan area.

Previous studies have suggested that the mineralization depths of skarn-type and quartz vein-type tungsten-molybdenum deposits are typically 2–4 km [62–64]. Zircon and apatite fission track data for the Tiechanghe granite indicate that the granite body was exhumed to approximately 2170 m [34], which is within the depth range at which tungsten-molybdenum deposits form. This suggests that the tungsten-molybdenum deposits in this area may have experienced uplift and erosion. Field geological surveys have revealed the presence of large quantities of tungsten minerals in the colluvial deposits below the skarn-type scheelite bodies, providing evidence that erosion has affected these mineralized bodies [35].

Therefore, exploration of tungsten-molybdenum-copper deposits should be intensified around the Tiechanghe granite body. Additionally, the impact of the uplift and erosion in the Jiulong area should be considered as tungsten-molybdenum-copper deposits may have been significantly eroded and lost due to uplift and exposure [35]. This finding offers new insights for mineral exploration in the Jianglang area and its surrounding regions. In summary, the focus of molybdenum-polymetallic exploration in the Tiechanghe region should be within 2–3 km of the Yanshanian (ca. 160 Ma) granite

 doi:10.20944/preprints202408.0432.v1

bodies, and careful attention should be paid to the effects of tectonic uplift and erosion on mineral exposure and preservation. This understanding can be applied to the entire western Sichuan region.

7. Conclusion

(1) The formation age of the Zierzi molybdenum-polymetallic deposit was determined to be 160.3 ± 1.6 Ma. This age is consistent with the Tiechanghe granite LA-ICP-MS U-Pb zircon ages (162–164 Ma) within the error range, indicating that a molybdenum mineralization event associated with granitic activity occurred at ca. 160 Ma.

(2) The emplacement and mineralization ages of the Tiechanghe granite and the tungsten-molybdenum deposits correspond to the peak of lithospheric extension in the southern margin of the Songpan-Ganzi Block. They represent the transition from the Indosinian compressional to the Yanshanian extensional tectonic environment in the Songpan-Ganzi Block. This transition also reflects the occurrence of shallow emplacement and mineralization in response to the regional tectonic shift from the Tethyan to the Pacific tectonic domain in the Jiulong area.

(3) The focus of the exploration for molybdenum-polymetallic deposits related to the Yanshanian (circa 160 Ma) granites in the Jiulong area in western Sichuan should be concentrated within 2–3 km of the granite bodies. It is also crucial to consider the impact of structural uplift on the degree of erosion, which affects the exposure and preservation of mineral deposits.

Author Contributions: S.Y.: Writing-original draft, Field collection sample, Data curation. H.T.: Field collection sample, Project administration. Z.L.: Review & editing. J.H.: Investigation, Formal analysis. X.W.: Figures editing, Formal analysis. L.D.: Field mapping, Formal analysis. All authors have read and agreed to the published version of the manuscript.

Funding: This work is funded by the National Natural Science Foundation of China (Grant No. 41603034), the China Geological Survey (Grant No.DD20160074, Grant No.DD20190185), and the Sichuan Science and Technology Plan (Grant No.2022YFS0488).

Data Availability Statement: The authors confirm that the data supporting the findings of this study are available within the article.

Declaration of Competing Interest: The authors declare no known competing financial interests or personal relationships that could have appeared to influence the work reported in this paper.

Acknowledgments: The zircon U-Pb dating was conducted with the assistance of the Continental Dynamics Laboratory at Northwest University. The molybdenite Re-Os dating was completed by Researcher Li Chao at the National Testing Center. Drs. Huadong Gong is appreciated for helping with the LA-ICP-MS zircon U-Pb analyses. We thank the editor and reviewers for their constructive remarks.

References

1. Wu: F.Y.; Liu, X.C.; Ji, W.Q.; Wang, J.M.; Yang, L. Discussions on the petrogenesis of granites. Acta Petrologica Sinica. 2007,23,1217-1238.
2. Wu, F.Y.; Liu, X.C.; Ji, W.Q.; Wang, J.M.; Yang, L. Highly fractionated granites: Recognition and research. Science China Earth Sciences. 2017,60,1201-1219.
3. Wang, X.L. Some new research progresses and main scientific problems of granitic rocks. Acta Petrologica Sinica. 2017,33,1445-1458.
4. Wang, T.; Wang, X.X.; Guo, L.; Zhang, L.; Tong, Y.; Li, S.; Huang, H.; Zhang, J.J. Granitoid and Petrologica Sinica. Acta Petrologica Sinica. 2017,33,1459-1478.
5. Xu, X.S.; Wang, X.L.; Zhao, K.; Du, D.H. Progresses and Tendencies of Granite Researches in Lase Decade: A Review. Bulletin of Mineralogy, Petrology and Geochemistry. 2020,39,899-911,1069.
6. Hu, J.M.; Meng, Q. R.; Shi, Y.R.; Qu, H.J. SHRIMP U-Pb dating of zircons from granitoid bodies in the Songpan-Ganzi terrane and its implications. Acta petrological Sinica.2005,21,867-880.
7. Zhang, H.F.; Parrish, R.; Zhang, L.; Xu, W. C.; Yuan, H.L.; Gao, S.; Crowley, Q.G. A-type granite and adakitic magmatism association in Songpan-Garze fold belt, eastern Tibetan Plateau: Implication for lithospheric delamination. Lithos.2007, 97,323-335.
8. Zhang, H.F.; Zhang, L.; Harris, N.; Jin, L.L.; Yuan, H. U-Pb zircon ages, geochemical and isotopic compositions of granitoids in Songpan-Garze Fold Belt, eastern Tibet Plateau: constraints on petrogenesis and tectonic evolution of the basement evolution of the basement. Contributions to Mineralogy and Petrology. 2006,152,75-88.

9. Weislogel, A.L. Tectonostratigraphic and geochronologic constraints on evolution of the northeast Paleo Tethys from the Songpan-Ganzi complex, central China. Tectonophysics. 2008,451,331-345.
10. Xiao, L.; Zhang, H. F.; Clemens, J.D.; Wang, Q. W.; Kan, Z.Z.; Wang, K.M.; Ni, P.Z.; Liu, X. M. Late Triassic granitoids of, the eastern margin of the Tibetan Plateau: Geochronology, petrogenesis and implications for tectonic evolution. Lithos.2007,96,436-452.
11. Yuan, C.; Zhou, M.F.; Sun, M.; Zhao, Y.J.; Wilde, S.; Long, X.P.; Yan, D.P. Triassic granitoids in the eastern Songpan Ganzi Fold Belt, SW China: Magmatic response to geodynamics of the deep lithosphere. Earth and Planetary Science Letters.2010,290, 481-492.
12. Cai, H.M.; Zhang, H.F.; Xu, W.C.; Shi, Z.L.; Yuan, H.L. Petrogenesis of Indosinian volcanic rocks in Songpan-Garze fold belt of the northeastern Tibetan Plateau: New evidence for lithospheric delamination. Sci China Earth Sci. 2010,53,1316-1328.
13. Roger, F.; Jolivet, M.; Malavieille, J. The tectonic evolution of the Songpan-Ganzê(North Tibet) and adjacent areas rom Proterozoic to Present: A synthesis. Journal of Asian Earth Sciences. 2010,39,254-269.
14. Roger, F.; Malavieille, J.; Leloup, P.H.; Calassou, S.; Xu, Z. Timing of granite emplacement ancooling in the Songpan-Garze fold belt (eastern Tibetan plateau) with tectonic implication. Jour nal of Asian Earth Science. 2004,22, 465-481.
15. Sigoyer, J.D.; Vanderhaeghe, O.; Duchêne, S.; Billerot, A. Generation and emplacement of Trias sic granitoids within the Songpan Ganze accretionary-orogenic wedge in a context of slab retreat accommodated by tear faulting, eastern Tibetan plateau, China. Journal of Asian Earth Sciences. 2014,88,192-216.
16. Chen, Q.; Sun; M.; Zhao, G.C.; Yang, F.L.; Long, X.P.; Li, J.H.; Wang, J.; Yu, Y. Origin of the mafic microgranular enclaves (MMEs) and their host granitoids from the Tagong pluton in Songpan–Ganze terrane: An igneous response to the closure of the Paleo-Tethys Ocean. Lithos. 2017,290-291,1-17.
17. Liu, D.M. Geochemical Composition, Chronology and Tectonic Significances of Sanyanlong-Galazi Granites in the Southern Songpan-Garze orogenic Belt (dissertation for master degree). Supervisor: Yin F G. Chengdu: Chengdu University of Technology. 2018,60p.
18. Yue, X.Y.; Guo, J; Mao, S.L.; Zhu, Z.M.; Tan, H.Q. Zircon U-Pb Age and Geochemistry of the Taiyanghe Granitoid in Western Sichuan, China and Its Geological Significance. Bulletin of Mineralogy, Petrology and Geochemistry. 2018,37,1142-1151.
19. Zhao, H.N.; Zhang, Y.Y.; Li, Q.G.; Du, W.; Zhang, Y.; Guo, Z.J. Early Jurassic I-type garnet leucogranite in the Siguniangshan pluton, eastern margin of the Songpan-Ganze terrane (NE Tibet), and its tectonic implications. Journal of Asian Earth Sciences.2020,188,104079.
20. Fei, G.C.; Menuge, J.F.; Li, Y.Q.; Yang, J.Y.; Deng, Y.; Chen, C. S.; Yang, Y. F.; Yang, Z.; Qin, L.Y.; Zheng, L.; Tang, W.C. Petrogenesis of the Lijiagou spodumene pegmatites in Songpan–Garze Fold Belt, West Sichuan, China: Evidence from geochemistry, zircon, cassiterite and coltan U-Pb geochronology and Hf isotopic compositions. Lithos.2020,364-365,1-18.
21. Yan, Q.G.; Li, J. K.; Li, X.J.; Liu, Y.C.; Li, P.; Xiong, X. Source of the Zhawulong granitic pegmatite-type lithium deposit in the Songpan-Ganzê orogenic belt, Western Sichuan, China: Constraints from Sr-Nd-Hf isotopes and petrochemistry. Lithos. 2020,378-379,1-11.
22. Zhan, Q.Y.; Zhu, D.C.; Wang, Q.; Weinberg, R.F.; Xie, J.C.; Li, S.M.; Zhang, L.L.; Zhao, Z.D. Source and pressure effects in the genesis of the Late Triassic high Sr/Y granites from the Songpan-Ganzi Fold Belt, eastern Tibetan Plateau. Lithos.2020,368-369, 1-15.
23. Ye, Y.K.; Zhou, J.Y.; Zhou, X.; Analysis, R. Zircon LA-ICP-MS U-Pb age and geochemical features of the Songlinkou pluton western Sichuan. Rock and Mineral Analysis.2020,39,921-933.
24. Tan, H.Q.; Zhu, Z.M.; Zhou, X.; Hu, J.L. Two Periods Rare Metal Mineralization of the Pegmatite in Jiulong Area, Western Sichuan. Multipurpose Utilization of Mineral Resources. 2022, 15-24.
25. Tan, H.Q.; Lü, F.Q.; Li, C.; Zhou, X.; Zhou, Y.; Liu, Y.D.; Hu, J.L.; Zhu, Z.M. Genetic linking with pegmatite-type veined molybdenum deposit and Dichishan highly differentiated granite in western Sichuan. Earth Science. 2023, 48, 3978-3994.
26. Tan, H.Q.; Zhu, Z.M.; Luo, L. H.; Hu, J.L. Distribution of early Yanshanian granite and its constraints on the mineralization of rare metals in Luomo area, western Sichuan. Acta Geologica Sinica. 2023, 97, 307-327.
27. Hu, J.L.; Tan, H.Q.; Ni, Z.Y.; Zhou, J.Y.; Zhu, Z.M.; Zhou, X.; Luo, Z.H.; Yue, X.Y.; Niu, T.; Xu, L.; et al. Geochemical characteristics, zircon U- Pb ages and Hf isotopic compositons of Baitai granite in Jiulong area, western Sichuan, and their significance for rear metals mineralization. Geological Review. 2024, 70, 449-475.
28. Wallis, S.; Tsujimori, T.; Aoya, M.; Kawakami, T.; Terada, K.; Suzuki, K.; Hyodo, H. Cenozoic and Mesozoic metamorphism in the Longmenshan orogeny: Implication for geodynamic model of eastern Tibet. Geology. 2003, 31, 745-758.
29. Zhou, J.Y.; Tan, H.Q.; Gong, D.X.; Zhu, Z.M.; Luo, L.P. Zircon LA-ICP-MS U-Pb dating and Hf isotopic composition of Xinhuoshan granite in the core of Jianglang dome, Western Sichuan, China. Mineralogy and Petrology. 2013, 33, 42-52.

30. Zhou, J.Y.; Tan, H.Q.; Gong, D.X.; Zhu, Z.M.; Luo, L.P. Wulaxi Aluminous A-type Granite in Western Sichuan，China: Recording Early Yanshanian Lithospheric Thermo-upwelling Extension of Songpan-Garze Orogenic Belt. Geological review. 2014, 60, 348-362.
31. Li, T.Z.; Dai, Y.P.; Ma, G.T.; Zhou, Q. SHRIMP Zircon U-Pb Dating of the Wulaxi Granite in the Western Margin of the Yangtze Block and Its Geological Significance. Bulletin of Mineralogy. Petrology and Geochemistry. 2016,35, 743-749.
32. Dai, Y.P.; Zhu, Y.D.; Li, T.Z.; Zhang, H.H.; Tang, G.L.; Shen, Z.W. A crustal source for ca. 165 Ma post-collisional granites related to mineralization in the Jianglang dome of the Songpan-Ganzi Orogen, eastern Tiebtan Plateau. Geochemistry. 2017, 77, 573-586.
33. 33 Zhu, Y.D.; Dai, Y.P.; Wang, L.L.; Li, T.Z.; Zhang, H.H.; Shen, Z.W. Petrogenesis and Geological Significance of the Wenjiaping Granite in Jianglang Dome, Southern Rim of Songpan-Garze Orogenic Belt. Geoscience. 2018,32,16-27.
34. Tan, H.Q. The composition, deformation-metamorphic characteristics and metallogenic response of the dome geological bodies on the south margin of Songpan-Garze Block (dissertation for doctor degree). Supervisor: Ni Z Y．Chengdu：Chengdu University of Technology. 2019,194-195p.
35. 35 Tan, H.Q.; Zhu, Z.M.; Zhou, J.Y.; Zhou,X.; Hu J.L.; Liu, Y.D. Early Yanshanian skarn W-Mo deposit in the southern margin of Songpan-Ganze terrane: Evidence from diagenetic and metallogenic chronology, zircon Hf isotopes in Daniuchang area. Mineral Deposits. 2022,41,53-58.
36. Liu, J; Li, W.C.; Zhou, Q.; Zhang, H.H. Late Jurassic Wenjiaping high Sr/Y granite: A product of partial melting of the Precambrian basement rocks trigged by lithospheric extension in the Songpan-Garze fold belt, SW China. Geological Journal. 2022, 57,4370-4387.
37. Zhang, H.C.; Zhou, H.B.; Yan, B. Determination of Yanshanian granite and its geological significance in the Taka Dome, Western Sichuan. Multipurpose Utilization of Mineral Resources. 2024, 45,1-7.
38. Xu, L. Chronology, Geochemistry and Tectonic Significance of the Lanniba Granites in Jiulong, West Sichuan (dissertation for Master degree). Supervisor: He Z W．Chengdu：Chengdu University of Technology. 2023,78p.
39. Huang, C.X. Study on the Ore-forming Fluid and Mineralization of the Hede W-Sn Deposit, Western Sichuan (dissertation for Master degree). Supervisor: Yang Y L and Tan H Q．Chengdu：Chengdu University of Technology. 2024,55p.
40. Zhou, M.F.; Yan, D.P.; Kennedy, A.K.; Li, Y.Q.; Ding, J. SHRIMP U-Pb zircon geochronological and geochemical evidence for Neoproterozoic, arc-magmatism along the western margin of the Yangtze block, south China. Earth and Planetary Science Letters.2002,196, 51-67.
41. Chen, Q.; Sun, M.; Long, X.P.; Yuan, C. Petrogenesis of Neoproterozoic adakitic tonalites and high-K granites in the eastern Songpan-Ganze fold belt and implications for the tectonic evolution of the western Yangtze Block. Precambrian Research. 2015, 170, 181-203.
42. Gong, D.X.; Wu, C.H.; Zou, H.; Zhou, X.; Zhou, Y.; Tan, H.Q.; Yue, X.Y. Provenance analysis of Late Triassic turbidites in the eastern Songpan–Ganzi flysch complex: sedimentary record of tectonic evolution of the eastern Paleo-Tethys ocean. Marine and Petroleum Geology. 2021,126,104927.
43. Liu, D.M.; Tan, H.Q.; Zhu, Z.M.; Yao, H.Y.; Yu, L. Tectonic setting and provenance of the Xikang Group in the Guining area, West Sichuan Province: Constraints from geochemistry of clastic sedimentary rocks. Geological Bulletin of China. 2021,40, 2135-2148.
44. Wan, C.H.; Yuan, J.; Li, F.X.; Yan, S.W. Late Triassic Granitoids in the Southern Part of the Songpan-Garze Fold Belt: Petrology, Geochemical Composition and Petrogenesis. Acta Petrologica et Mineralogica. 2011, 30,185-198.
45. Yuan, J.; Xiao, L.; Wan, C.H.; Gao, R. Petrogenesis of Fangmaping-Sanyanlong Granites in Southern Songpan-Garze Fold Belt and Its Tectonic Implication. Acta Geologica Sinica. 2011,85,195-206.
46. Hu, J.L.; Tan, H.Q.; Zhou, X.; Nii, Z.Y.; Zhou, Y. A study of mineralogy and mineral chemistry of ore-bearing pegmatites in the Daqianggou lithium-beryllium deposit, western Sichuan. Geological Bulletin of China. 2020,39,2013-2028.
47. Liu, Y.D.; Xie, H.F.; Xu, L.; Ni, Z.Y.; Lü, F.Q.; Tan, H.Q. Sulfur isotopic geochemistry of the Zigangping Pb-Zn deposit, Jiulong County, Sichuan Province. Geological Bulletin of China. 2020,39, 2029-2036.
48. Zhou, Q.; Li, W.C.; Zhang, H.H.; Li, T.Z.; Yuan, H.Y.; Feng, X.L.; Li, C.; Liao, Z.W.; Wang, S.W. Post-Magmatic Hydrothermal Origin of Late Jurassic Liwu Copper Polymetallic Deposits，Western China: Direct Chalcopyrite Re-Os Dating and Pb-B Isotopic Constraints. Ore Geology Reviews. 2017, 89, 526-543.
49. Zhou, Q.; Li, W.C.; Zhang, H.H.; Li, T.Z.; Dai, Y.P.; Liu, J.; Yang, B.; Shen, Z.W.; Wang, C.N.; Tang, G.L. Two pulses of metallogenesis of the Liwu Stratiform-like Cu-Rich polymetallic Deposit, western China: Evidence from geology, Re-Os dating and lead isotope. Ore Geology Reviews. 2023, 156, 105373.
50. Li, T.Z.; Zhou, Q.; Zhang, H.H.; Dai, Y.P.; Ma, G.T.; Ma, D.; Shen, Z.W. Ore Geology and Molybdenite Re-Os dating of the Wulaxi Tungsten Deposit in Western Sichuan. Geological Journal of China Universities. 2016, 22, 423-430.

51. Yuan, H.L.; Gao, S.; Liu, X.M.; Li, H.M.; Günther, D.; Wu, F.Y. Accurate U-Pb Age and Trace Element Determinations of Zircon by Laser Ablation-Inductively Coupled Plasma Mass Spectrometry. Geostand. Newsl, 2004, 28, 353-370.
52. Wiedenbeck, M.; Hanchar, J.M.; Peck, W.H.; Sylvester, P.; Valley, J.; Whitehouse, M.; Kronz, A.; Morishita, Y.; Nasdala, L.;Fiebig, J.; et al. Further characterisation of the 91500 zircon crystal. Geostand. Geoanal. Res. 2004. 28, 9–39.
53. Ludwig, K.R. User's Manual for isotopic 3.0: A Geochronological Toolkit for Microsoft Excel. Berkeley: Berkeley Geochronology Center. 2003, Special Publication.No.4. 25-32p.
54. Du, A. D.; Wu, S. Q.; Sun, D. Z.; Wang, S. X.; Qu, W. J.; & Markey, R.; et al. Preparation and certification of re-os dating reference materials: molybdenites hlp and jdc. Geostandards and geoanalytical research(1), 2004, 28.
55. Ferry, J.M.; Watson, E.B. New Thermodynamic Models and Revised Calibrations for the Ti-in-zircon and Zr-in-rutile Thermometers. Contrib. Mineral Petrol, 2007, 154, 429–437.
56. Liu, Y.P.; Li, Z.X.; Li, H.M.; Guo, L.G.; Xu, W.; Ye, L.; Li, C.Y.; Pi, D,H. U-Pb Geochronology of Cassiterite and Zircon from Dulong Sn-Zn Deposit: Evidence for Cretaceous Large-Scale Granitic Magmatism and Mineralization Events in Southeastern Yunnan Province, China. Acta Petrologica Sinica.2007,23,967-976.
57. Tan, H.Q.; Liu, Y.P.; Xu, W.; Guo, L.G.; Ye, L.; Li, C.Y. 40Ar-39Ar dating of Phlogopite from W-Sn deposits in the Nanyangtian，southeastern Yunnan，and its implication. Acta Mineralogica Sinica. 2011, 31,639-640.
58. Liu,Y.; Deng, J.; Shi, G. H.; Sun, X.; Yang, L.Q. Genesis of the Xuebaoding W-Sn-Be crystal deposits in Southwest China: Evidence from fluid inclusions, stable isotopes and ore elements. Resour. Geol. 2012, 62, 159-173.
59. Liu, Y.; Deng, J.; Li, C.F.; Shi, G.H.; Zheng, A.L. REE composition in scheelite and scheelite Sm-Nd dating for the Xuebaoding W-Sn-Be deposit in Sichua. Chinese Science Bulletin. 2007,52, 2543-2550.
60. Tan, H.Q. Re-Os dating of molybdenites and its geological significance in the Jianglang dome, SW China. Acta Geologica Sinica. 2014, 88, 928.
61. Xu, Z. Q.; Hou, L. W.; Wang, Z.X.; Fu, X.F.; Huang, M.H. Orogenic process of Songpan-Ganzi orogenic belt in China. Beijing: Geol. Pub. House. 1992,170-182p.
62. Liu, X.J.; Xu, Z.Q. Tectonic significance of Middle Jurassic granite in the Jianglang dome, southern Songpan-Ganzi orogen belt. Acta Geological Sinica. 2021, 95,1754-1773.
63. Boehnke, P.; Trail, D.; Schmitt, A.K.; Watson, E.B.; Harrison, M. Zircon saturation re-revisited. Chemical Geology, 2013, 351, 324-334.
64. Ren, Y.S.; Liu, L. D.; Wan, X.Z.; Liu, L.G. Discussion on the metallogenic depth of skarn type gold deposits in Tongling area, Anhui province. Geotectonica et Metallogenia. 2004,28,397-403.
65. Ding, C.G.; Zhang, S.G; Ma, C.; Xu, Z.F. Genetic mineralogical properties of sphalerite and discussions on its geobarometer application in skarn ore deposits in middle Ningzhen region. Journal of Geology. 2009,33,124-129.
66. Tian, K.; Zheng, Y.Y.; Gao, S.B.; Wu, D.H.; Jiang, X. J. Fluid Source and Evolution of the Bangbule Skarn Pb-Zn-Cu-Fe Deposit in Tibet: Constraints from Fluid Inclusions and Stable Isotopes. Geotectonica et Metallogenia. 2018,42,1027-1045.